

Ostracods, rock facies and magnetic susceptibility records from the stratotype of the Terres d'Haurs Formation (Givetian) at the Mont d'Haurs (Givet, France)

by Jean-Georges CASIER, Xavier DEVLEESCHOUWER, Julien MOREAU, Estelle PETITCLERC & Alain PRÉAT

CASIER, J.-G., DEVLEESCHOUWER, X., MOREAU, J., PETITCLERC, E. & PRÉAT, A., 2011 – Ostracods, rock facies and magnetic susceptibility records from the stratotype of the Terres d'Haurs Formation (Givetian) at the Mont d'Haurs (Givet, France). *Bulletin de l'Institut royal des Sciences naturelles de Belgique, Sciences de la Terre*, 81: 97-128, 6 pls, 5 figs, 2 tables, Brussels, November 30, 2011 – ISSN 0374-6291.

Abstract

More than 5,500 carapaces, valves and fragments of ostracods, were extracted from 48 samples collected in the stratotype of the Terres d'Haurs Formation (= Fm) and in the very base of the stratotype of the Mont d'Haurs Fm, at the Mont d'Haurs, close to Givet. Fifty-two species belonging to several assemblages of the Eifelian Mega-Assemblage have been identified. They are generally indicative of neritic marine environments below fair-weather wave base, some even below storm wave base. Ostracods indicative of semi-restricted environments are also present but the sedimentological analysis displays that these ostracods have been mainly transported from these shallow settings. Close to the boundary of the Terres d'Haurs Fm and the Mont d'Haurs Fm, thick-shelled ostracods indicate that the energy of the environment increased. The richness in ostracods and their great diversity in the two studied sections prove that the living conditions were particularly favourable for these crustaceans.

Ten microfacies are recognized, the succession of which (from 1 to 10) constitutes a standard shallowing upward sequence, with environments ranging from open marine, near storm wave base, to coastal, close to subaerial exposure. The microfacies analysis points to a carbonate ramp system with oolitic shoals and algal shoals separating semi-restricted and coastal areas from the open marine environment. Storm events and those related to the wave activity redistributed many organisms, which formed diversified communities with abundant echinoderms, bryozoans, molluscs and brachiopods in the peri-shoal environments. The lithological curve reflects a progressive and transgressive evolution in two phases marked by two parasequence sets: the first set records the destabilization of the overlain carbonate platform (Trois-Fontaines Fm) leading to the establishment of a shallow “open lagoon” in the inner ramp, the second set corresponds to the development of several shoals at the inner-mid ramp zones. No important reefal episode is present and shoals are of modest relief. The salinity and energy were the key parameters controlling the zonation of the organisms and the distribution of the environments.

Low-field magnetic susceptibility (X_{LF}) values are weak and eight magnetic susceptibility evolutions are reported along the lithological column. The magnetic susceptibility and microfacies curves are more or less mimetic in the lower half of the section and opposite in the upper part of the Terres d'Haurs Fm. A significant decreasing trend of the low-field magnetic susceptibility values across the boundary between the Terres d'Haurs Fm and the Mont d'Haurs Fm is presented. Two linear regression models show a moderately positive correlation between X_{LF} values and microfacies in the lower half of the section and a moderately strong negative correlation between these two parameters in the upper part of the Terres d'Haurs Fm. The water agitation is highest in the mid and inner ramp, associated to the oolite and algal shoal environments and corresponds to the lowest mean X_{LF} values presented in the models. The lower half of the section corresponds more to a carbonate platform profile in opposition to the second model, which confirm the carbonate ramp morphology. The average X_{LF} values in the upper part of the Terres d'Haurs Fm are more homogeneous compared to those reported in the lower half of the Terres d'Haurs Fm. High-resolution stratigraphic correlation for the base of the Mont d'Haurs Fm in Belgium and France is proposed due to similar X_{LF} data established in the “Les Monts de Baileux” section 40 km distant from the stratotype area.

Keywords: Ostracods, Sedimentology, Palaeoecology, Magnetic Susceptibility, Givetian, Dinant Synclinorium, Ardennes, France.

Résumé

Plus de 5.500 carapaces, valves et fragments d'ostracodes ont été extraits de 48 échantillons récoltés dans le stratotype de la Formation (= Fm) des Terres d'Haurs et dans l'extrême base de la Fm du Mont d'Haurs, au Mont d'Haurs, près de Givet. Cinquante-deux espèces appartenant au Mega-Assemblage de l'Eifel sont reconnues, et elles indiquent généralement des environnements marins sous la zone d'action des vagues de beau temps et occasionnellement sous la zone d'action des vagues de tempêtes. Des ostracodes indicateurs d'environnements semi-restrints sont également reconnus mais l'analyse sédimentologique montre que parfois ces ostracodes ont été transportés. Au passage Fm des Terres d'Haurs / Fm du Mont d'Haurs, des ostracodes à carapaces épaisses témoignent d'une plus grande agitation des eaux. La grande abondance des ostracodes et leur grande diversité montrent que les conditions de vies étaient particulièrement favorable pour ces crustacés.

Dix microfaciès sont reconnus, leur succession de 1 à 10 correspond à une séquence standard de type ‘shallowing-upward’ depuis des milieux marins ouverts à proximité de la zone d’action des tempêtes jusqu’aux milieux littoraux proches de l’émergence. L’analyse des microfaciès met en évidence un système de rampe carbonatée avec des shoals oolithiques et algaires séparant un domaine semi-restrait et littoral du milieu marin franc. Les événements de tempêtes, et ceux liés à l’activité des vagues, redistribuent les organismes qui formaient des biocénoses diversifiées à échinodermes, bryozoaires, mollusques et brachiopodes dans les environnements d’avant-shoal. La courbe lithologique traduit une évolution transgressive progressive (cortège sédimentaire) en deux phases marquées par deux ensembles de paraséquences: le premier ensemble enregistre la déstabilisation de la plate-forme carbonatée sous-jacente (Fm de Trois-Fontaines) donnant lieu à la mise en place d’environnements de type lagunaires “ouverts” dans la rampe interne, le second ensemble correspond à l’installation des shoals à la limite rampe interne/médiane. Aucun épisode récifal important n’est présent, et les shoals sont de relief modeste. La salinité et l’énergie sont les paramètres majeurs qui déterminent les zonations d’organismes et la répartition des environnements.

Les valeurs de susceptibilité magnétique en champ faible (X_{LF}) sont faibles et huit évolutions de susceptibilité magnétique sont reportées face à la colonne lithologique. Les courbes de susceptibilité magnétique et de microfaciès sont relativement mimétiques dans la première moitié de la coupe et opposées dans la partie supérieure de la Formation des Terres d’Haurs. Une tendance décroissante des valeurs de SM en champ faible à travers la limite entre les formations de Terres d’Haurs et de Mont d’Haurs est observée. Deux modèles de régression linéaire sont proposés dont l’un montre une corrélation positive modérée entre les valeurs X_{LF} et les microfaciès dans la première moitié de la coupe et le deuxième est caractérisé par une corrélation négative forte entre ces deux paramètres pour la partie supérieure de la Fm des Terres d’Haurs. L’agitation de l’eau est la plus élevée dans la rampe interne et médiane en association avec les environnements de shoals oolithiques et algaires et correspond aux valeurs les plus faibles des valeurs en X_{LF} . La partie inférieure semble correspondre plus à un profil de plateforme carbonatée par opposition au second modèle qui confirme une morphologie de rampe carbonatée. Les valeurs moyennes de X_{LF} observées dans la partie supérieure de la Fm des Terres d’Haurs sont relativement homogènes comparées aux fluctuations reportées dans la moitié inférieure de la coupe. Une corrélation stratigraphique à haute résolution est proposée pour la base de la Fm du Mont d’Haurs en Belgique et en France en raison d’une similitude des données de X_{LF} établies pour la coupe des Monts de Baileux située à quarante kilomètres de distance du stratotype.

Mots-clés: Ostracodes, Sédimentologie, Paléoécologie, Susceptibilité Magnétique, Givétien, Synclinorium de Dinant, Ardennes, France.

Introduction

This paper is part of a series on Middle Devonian ostracods and their lithological context in the type region of the Givetian Stage (southern part of the Dinant Synclinorium). In a first paper (CASIER *et al.*, 2011), we studied the boundary between the Hanonet Formation (Fm) and the Trois-Fontaines Fm (Early

Givetian) in a section located along the southwestern rampart of the historically entrenched military camp at the Mont d’Haurs (Ardennes Department, France) (Fig. 1, section 1). In a second paper (CASIER *et al.*, 2010) we studied the boundary between the Trois-Fontaines Fm and the Terres d’Haurs Fm (also Early Givetian), exposed in the Rancennes Quarry along the western rampart of this military camp (Fig. 1, section 2). In the scope of these two studies, 292 samples were collected for sedimentology and magnetic susceptibility (MS), and 90 others for ostracod investigation.

As shown in the two publications mentioned above, the upper part of the Hanonet Fm records a mixed silico-carbonate ramp setting. Peloidal silty packstones rich in *Girvanella* and cricoconarids are associated with crinoidal packstones-grainstones, and coral and stromatoporoid floatstones-rudstones suggesting mid- and inner ramp palaeoenvironments. These open marine environments were occasionally subjected to a high-energy regime that destroyed the crinoidal meadows and the bioconstructions, which were subsequently deposited as numerous proximal and distal tempestites. The transition to the overlying lagoonal facies of the Trois-Fontaines Fm, dominated by calcispheres, cyanobacteria and paleosiphonocladales, is abrupt and the environment changed to very shallow, restricted, intertidal to supratidal, with loferites in slightly evaporative conditions. These microfacies are typical for the Trois-Fontaines Fm and characterize a very shallow restricted carbonate platform, which evolves to a mixed ramp in the base of the overlying Terres d’Haurs Fm. More than 2,000 ostracods were extracted, and 69 species belonging to the Eifelian Mega-Assemblage have been identified in sections 1 and 2. A generally good correlation is observed between the results obtained by the ostracod study, the sedimentological analysis and the magnetic susceptibility (MS in what follows) investigation. Especially in the Trois-Fontaines Fm, there is a correspondence between the highest MS values, the restricted environments displayed by the sedimentological analysis and the occurrence of Leperditicopida, indicator of lagoonal environments.

This paper, the third of the series on the Givetian in its type region, focuses on the stratotype of the Terres d’Haurs Fm, the second formation in the Givet Group, and on the base of the overlying Mont d’Haurs Fm. Two sections, numbered 3 and 4, have been selected (see Fig. 1). Section 3 is located in a passage along the southern rampart of the military camp (from N50°07'37,3"; E4°49'51,0" to N50°07'39,2"; E4°49'54,5") and exposes the middle part of the Terres

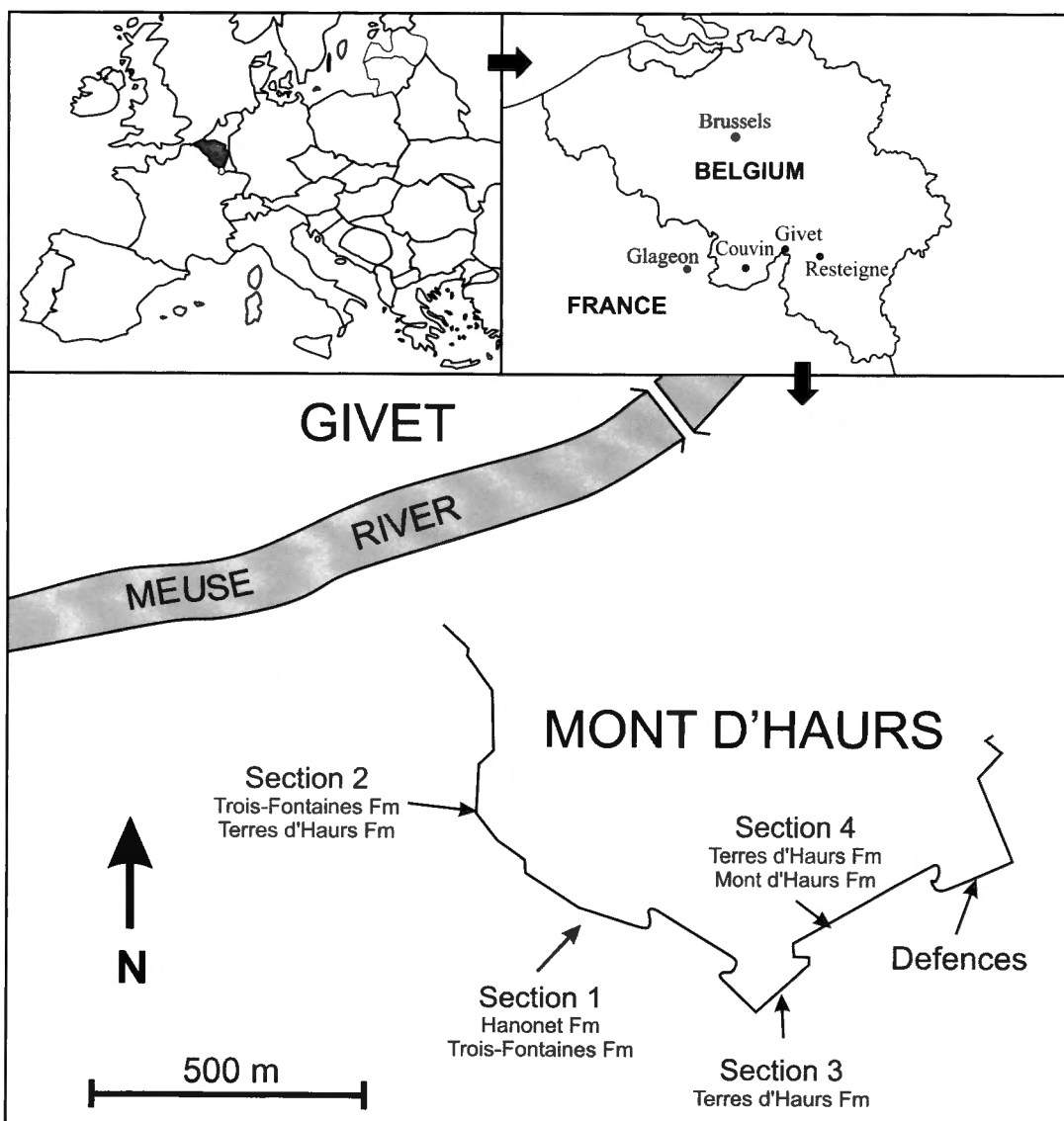
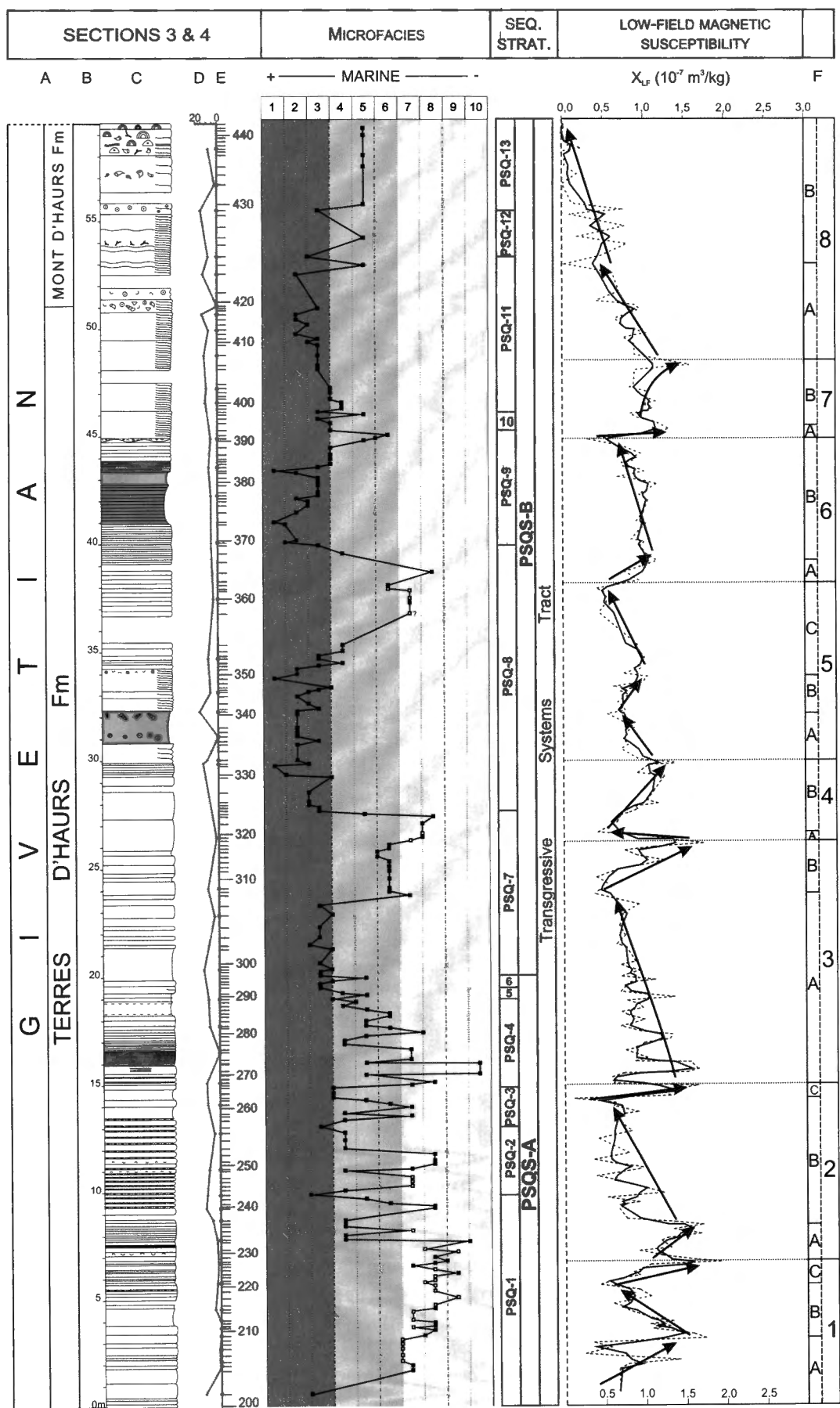


Fig. 1 – Locality map of sections 3 and 4 along the south-western rampart of the historically entrenched military camp at the Mont d'Haurs. Section 1 exposes the transition from the Hanonet Fm to the Trois-Fontaines Fm (see: CASIER *et al.*, 2011, this bulletin) and section 2 exposes the boundary between the Trois-Fontaines Fm and the Terres d'Haurs Fm (see: CASIER *et al.*, 2010).

d'Haurs Fm (samples MH-201 to MH-405). Section 4 is situated in a trench located on both sides of the entry of a subway in the fortification ($N50^{\circ}07'40,6''$; $E4^{\circ}49'54,7''$) and exposes the upper part of the Terres d'Haurs Fm (samples MH-406 to MH-418) and the base of the Mont d'Haurs Fm (samples MH-419 to MH-443). The Terres d'Haurs Fm is approximately 70 m thick and is composed of dark argillaceous carbonates, locally with crinoids and scarce bioclastic thin beds, rich in corals (PRÉAT & TOURNEUR *in* BULTYNCK *et al.*, 1991). The base is characterized by massive rugose-rich beds, although not exposed in the zone studied herein (HUBERT, 2008). About 9 meters are missing

in section 3. In order to complete the stratotype of the Terres d'Haurs Fm we studied its lower part in the Rancennes Quarry (Fig. 1, section 2) (CASIER *et al.*, 2010). The totality of the Terres d'Haurs Fm belongs to the *timorensis* conodont Zone (BULTYNCK, 1987; BULTYNCK & DEJONGHE, 2001) and, consequently, is Early Givetian in age.

The Givetian at the Mont d'Haurs has been the subject of numerous papers (See: ERRERA *et al.*, 1972, and BULTYNCK *et al.*, 1991, for an exhaustive bibliography) and recently HUBERT (2008) published a paper on the lithology and the faunal occurrences at the Mont d'Haurs.



LITHOSTRATIGRAPHIC LOG LEGEND					
MASSIVE STROMATOPORES	LIMESTONE	—	LOW-FIELD MAGNETIC SUSCEPTIBILITY (X_{LF})		
LAMELLAR STROMATOPORES	ARGILLACEOUS LIMESTONE	—	3-PERIOD SIMPLE MOVING AVERAGE ON X_{LF}		
TABULATE CORALS (BRANCHING)	A STRATIGRAPHY	F	MAGNETIC SUSCEPTIBILITY EVOLUTION		
TABULATE CORALS (MASSIVE)	B METRIC SCALE	?	UNCERTAIN MICROFACIES		
CRINOIDS	C LITHOLOGICAL COLUMN	□	BRINE REFLUX (DIAGENESIS)		
BRACHIOPODS	D NUMBER OF OSTRACOD SPEC.	x	NO THIN SECTION		
GASTROPODS	E SAMPLE POSITION				
BIOCLASTS	— SAMPLE (MS / THIN SECTION)				
CLAYEY LEVEL	— SAMPLE (OSTRACODS)				
LAMINAR STRATIFICATION					

Fig. 3 – Key to symbols used in Fig. 2.

Rock and facies analyses (A. PRÉAT & J. MOREAU)

The studied sections of the Terres d'Haur Fm expose nearly fifty meters of poorly thin- and medium-thick bedded fine- to medium-grained bluish clayey bioclastic wackestones and packstones. The transition to the overlying Mont d'Haur Fm, which outcrops over nearly 10 meters in section 4, is highlighted by apparition of massive beds with decimetric-sized stromatopores and corals (rugosa and tabulata) forming a biostrome (floatstones and rudstones) at the top of the section. The bedding of the series is regular with thin (millimetric to centimetric) argillaceous joints and diastems interstratified in these rather homogeneous limestones. Crinoids, various shell bioclasts (brachiopods, pelecypods, gastropods) and rare corals are the only distinguishable organisms observed in the Terres d'Haur Fm in the field. Two hundred and forty-four samples (MH200-MH443) have been collected (Figs 2-3) for petrography in order to constrain the paleoenvironments. It is clear from the field observation that the Terres d'Haur Fm represents a pronounced evolution from the restricted carbonate platform of the underlying Trois-Fontaines Fm towards an open-marine environment in a ramp setting (CASIER *et al.*, 2010).

As the transition from the Trois-Fontaines Fm to the Terres d'Haur Fm represents a transition from a mixed carbonate platform to a clayey-carbonate ramp system in the Dinant Basin (MABILLE, 2008; BOULVAIN *et al.*, 2009; CAMBIER, 2010), the microfacies distribution and evolution are rather complex and their key parameters changed through time. Such a complex microfacies evolution has already been described by PRÉAT &

KASIMI (1995) and CASIER *et al.* (2011) at the Eifelian/Givetian transition in the Dinant Basin. In these cases the sedimentary evolution concerned the transition from the Hanonet Fm to the Trois-Fontaines Fm, which appeared to correspond to a progressive shift from a mixed siliciclastic-carbonate ramp system to a carbonate platform (KASIMI & PRÉAT, 1996). Despite these two different sedimentary evolutions the standard sequences highlight a similar shallowing-upward trend from subtidal open-marine environments near storm wave base level to supratidal settings with emerged surfaces. PRÉAT & KASIMI (1995) proposed a standard sequence of ten major microfacies based on the energy index variation from open-marine (below storm wave base level) to reefal complexes, open lagoons and peritidal environments near emerged surface with vadose cavities.

Microfacies analysis (Table 1)

Open-marine below storm-wave base

Microfacies type I (MF1) (Pl. 4, Figs 1-2)

Description: this microfacies is not well represented and has not been systematically sampled due to its relatively important clay content. It occurs in the middle part of the formation and consists of centimetric and decimetric homogeneous clayey silty mudstones and wackestones. Under the microscope bioclasts are rather diverse and consist of well-preserved crinoids, sea urchins (spines), trilobites, molluscs and ostracods and they occasionally form thin bioclastic laminae less than one millimetre thick. Rare bryozoans and algae are observed. Bioturbation is present as well as vortex

Fig. 2 – Lithological column, microfacies, lithological curve and magnetic sequence of sections 3 and 4, Terres d'Haur Fm and base of Mont d'Haur Fm at the Mont d'Haur, Givet (France). (A) and (B) stratigraphy; (C) lithology; (D) number of ostracod species; (E) position of samples for ostracods (black dots), thin sections and MS analysis. The dashed line corresponds to raw low-field magnetic susceptibility values ($10^{-7} \text{ m}^3/\text{kg}$) and the black line represents the 3-period simple moving average. See Fig. 3 for key symbols.

figures and well-delimited burrows often filled with peloids. Small-sized pyritic grains are observed as blackened grains *sensu* MAMET & PRÉAT (2005). This microfacies is equivalent to MF1 of PRÉAT & KASIMI (1995).

Interpretation: the well-preserved bioclasts and their nature suggest a quiet open-marine environment at the upper limit of the storm waves and at the dysphotic-euphotic boundary as suggested by the blackened grains and the rarely observed algae. The environment could correspond to that of an outer ramp setting (BURCHETTE & WRIGHT, 1992).

Open-marine environment near storm wave base, proximity of *Girvanella*-cyanobacterial mats

Microfacies type 2 (MF2) (Pl. 4, Figs 3-4)

Description: burrowed bioclastic and microbioclastic clayey silty wackestone. The fine-grained bioclasts mostly consist of crinoids and sea urchin fragments (spines and plates), brachiopods, occasional bryozoans, ostracods, molluscs, trilobites, algae (issinellids and kamaenids) and small-sized “floated” goniatites. Small-(20-30 µm) and larger-sized (80-100 µm) irregular peloids are present, the latter consisting of *Girvanella* fragments coming from associated *Girvanella*-oncoids. Same pyritic and blackened grains as in microfacies type 1 are observed. The laminations (less than one millimetre up to 1 mm thick) are generally destroyed by bioturbation, resulting in a bimodal size distribution of the bioclasts. Abundant well-delimited burrows developed in all directions and are filled with peloids. The matrix is sometimes a fine-grained calcite microspar. A large (plurimillimetric) saddle dolomite occurs in the molluscan shells. Pyrite accumulated in the irregular pressure solution seams.

Interpretation: the well-preserved bioclasts and their composition suggest a quiet open-marine environment, episodically interrupted by storm events as indicated by the occurrence of thin bioclastic layers (less than one millimetre thick). The *Girvanella* fragments point to the proximity of the euphotic zone. The environment could be compared with the transition zone described in the North Sea (German Bay) by AIGNER (1985). This microfacies belongs to the mid ramp setting *sensu* AHR (1973) and BURCHETTE & WRIGHT (1992).

Microfacies type 3 (MF3) (Pl. 4, Figs 5-8)

Description: burrowed wackestone and peloidal packstone with abundant and diversified medium-grained bioclasts (brachiopods, bryozoans, ostracods, molluscs, echinoderms, archaeogastropods, trilobites,

issinellids, kamaenids, *Girvanella*). Rare “floated” goniatites and calcispheres have also been recorded. Various grains are mixed in the matrix and consist of irregular small-sized peloids with *Girvanella* and microbreccias coming from oolitic and algal (codiaceans and triangulinellids) packstones. All bioclasts, including the coarser ones, are concentrated in interstratified centimetre thick packstone layers in the micritic matrix. Pyrite, blackened grains, saddle dolomite and bioturbation are identical to these observed in the previous microfacies. The matrix is slightly microsparitized and as a consequence is replaced by small-sized whitish calcite grains consisting of pseudomorphs of larger acicular crystals.

Interpretation: the abundance of the cyanobacterial or *Girvanella* fragments point to the proximity of a shoal colonized by microbial mats in the photic zone. The bioclastic packstone layers and the occurrence of coarse-grained bioclasts point to an environment exposed to episodic storms, which led to mixing of several biocenoses (*Girvanella*, brachiopods, etc.) in a shallow-water open-marine setting. These layers are comparable to intermediate and proximal tempestites described by AIGNER (1985). Blackened grains were formed in the dysoxic-anoxic zone at the sediment/water interface during early diagenesis (MAMET & PRÉAT, 2005) and were reworked by storm activity.

Open-marine fore-reef environment around the fair-weather wave base

Microfacies type 4 (MF4) (Pl. 5, Figs 1-4)

Description: laminar bioclastic wackestone, packstone and grainstone. The bioclasts are similar to those found in previous microfacies, although include abundant encrusting bryozoans. They are coarser and consist of colonial encrusting organisms (stromatoporoids and corals), leading in some cases to floatstones and rudstones. Oolites (200-500 µm) fill the burrows and poorly sorted subrounded microbreccias are common. They consist of oolitic packstones, silty mudstones-wackestones and sponge wackestones with abundant spicules. The laminae are plane-parallel or slightly oblique and plurimillimetre to centimetre thick. Algae are as common as in the previous microfacies.

Interpretation: the abundance of reworked organisms with a few stromatoporoids and corals mixed with echinoderms, brachiopods and bryozoans, points to a fore-shoal environment close to the euphotic zone as suggested by the presence of algae and cyanobacteria. This general high-energy “reefal” environment was exposed to episodic storms, which led to mixing of

Table 1 – Main characteristics of the microfacies standard sequence, from microfacies 1 to microfacies 10 in the Terres d’Haurs Fm, Lower Givetian, Mont d’Haurs, Givet (France).

	Texture	Composition	Particular features	Environment	Variety
MF-1	Argillaceous and silty bioturbated mudstone - wackestone	crinoids, sea urchins, ostracods, trilobites	Exceptional storm deposits	Outer ramp, under storm wave base, dysphotic-euphotic zone	-
MF-2	Burrowed (micro)bioclastic clayey silty wackestone - packstone	crinoids, sea urchins, ostracods, trilobites, brachiopods, reworked algae	Distal and intermediate storm deposits	Mid ramp, storm wave base, open marine	-
MF-3	Burrowed wackestone and peloidal packstone	Abundant bioclasts (including bryozoans) and high amount of shell deposits and reworked algae	Intermediate and proximal storm deposits	Mid ramp, storm wave base, open marine	-
MF-4	Laminar bioclastic wackestone, packstone and grainstone	Abundant bioclasts, with encrusting bryozoans; microbreccias, oolites and oncoids	Intermediate and proximal storm deposits, high energetic index and bimodal distribution of the bioclasts	Mid ramp, storm wave base; living environment for some organisms	Bioclastic peloidal packstone
MF-5	Floatstone - rudstone, ‘false’ grainstone	Abundant bioclasts, corals and stromatoporoids; microbreccias, oolites and oncoids	Proximal storm deposits, high energetic index; bimodal distribution of the bioclasts	Mid ramp, storm wave base; patch reefs and peri-shoals	Offshore channel with microbreccias and oolites
MF-6	Oolitic and peloidal packstone - grainstone and ‘false’ grainstone, cross stratifications	Bioclasts, crinoids, trilobites, Microbreccias, oolites and oncoids, nodular codiaceans; relicts of anhydrite.	High to moderate energetic index	Oolitic shoals, bottom of the fair-weather wave base	Bioclastic packstone with oolites
MF-7	Algal peloidal packstone - grainstone; cross stratifications and bioturbation	Reworked algae (issinellids, kamaenids) and diversified bioclasts	Moderate energetic index; bimodal distribution of the bioclasts	Reworking of MF-8; algal shoals in the fair-weather wave base	Storm shells deposits
MF-8	Issinellid bafflesstone, peloidal packstone - grainstone; ‘false’ grainstone	Algae, peloids, calcispheres	Low energetic index	Algae in the euphotic zone	Storm shells deposits and strong bioturbation
MF-9	Mudstone - wackestone	Algae, ostracods, gastropods, radial oolites	Low energetic index	Near emersion and isolated evaporites (pseudomorphs)	Storm shells deposits
MF-10	Mudstone with desiccation cracks and microfractures	Ostracods, intraformational microbreccias	Very low energetic index	Intra and supratidal channel environment; evaporites (laths of sulfate pseudomorphs)	-

several biocenoses. The grain size distribution of the bioclasts and the mixing of various subangular microbreccias points to proximal tempestites *sensu* AIGNER (1985).

Microfacies type 5 (MF5) (Pl. 5, Figs 5-6)

Description: floatstone and rudstone with abundant diversified coarse-grained bioclasts in relatively thick-bedded (0.5 – 2cm) packstone layers. The bioclasts are the same as in the above described microfacies with a significant increase of stromatoporoids, corals and reworked algae and cyanobacteria (*Girvanella*, *Issinella*, *Kamaena*, *Triangulinella tricarinata* MAMET & PRÉAT, 1985; see below). Cross-bedding and erosive discontinuities are present. *Bisphaera (Incertae sedis)* is observed for the first time. Oncoids with codiacean cortices, radial oolites, peloids and millimetric subangular microbreccias are regularly present. The micritic matrix of the floatstones is frequently replaced by a fine- and coarse-grained calcite microspar and the rock seems therefore similar to a “false” grainstone (*sensu* MAMET & PRÉAT, 2005). On the contrary true cementation, and therefore true grainstones, developed in the coquina levels interlayered in the rock. This is a consequence of the high intra- and interparticular primary porosities of the coquina levels.

Interpretation: same environment as suggested in microfacies 4, but more proximal as shown by coarser bioclasts. The environment was very close to the fair-weather wave base and can represent the subtidal part of an offshore channel fed by oolites coming from intertidal upstream areas. Sediment transport in channels may be most active during storms that generate off-bank currents (HINE *et al.*, 1981).

Open-marine shoals in the fair-weather wave base

Microfacies type 6 (MF6) (Pl. 5, Figs 7-8)

Description: oolitic and peloidal packstone and grainstone with cross-stratification and graded bedding. Bioclastic content is similar to previous microfacies with abundant reworked *Bevocastria* lumps. Micritized grains, *Bevocastria* and *Triangulinella*, constitute frequently the nuclei of the oolites. Oolites are well sorted, most commonly spherical, and their sizes (from 200 µm to 1 mm) are function of the size of their nuclei. Oolitic microbreccias are also present as other various subrounded microbreccias composed of algal and sponge packstones. The microbreccias are up to 1 cm in size. Bioturbation is not well developed and partly disrupted the laminae. Relicts of anhydrite are observed in the former intergranular pore space.

Interpretation: oolitic shoal or tidal bar in a moderate and temporarily high-energy environment as indicated by cross-bedding and abundance of microbreccias. The shoal sedimentation is the result of a mixing of bioclasts brought from the open marine environment, and algae and microbreccias coming from the back-shoal area where semi-restricted conditions prevailed.

Microfacies type 7 (MF7) (Pl. 6, Figs 1-2)

Description: algal (issinellids, kamaenids, triangulinellids) peloidal packstone and grainstone with diversified bioclasts (echinoderms, molluscs, brachiopods, serpulids and ostracods - with easy recognizable *Cryptophyllum*). The open marine fauna is significantly less abundant as compared with previous microfacies. Few bryozoans, archaeogastropods and calcispheres are present. The matrix of the packstone and the peloids (50-100 µm) contain small-sized bipyramidal quartz of the same type as those described by PRÉAT & MAMET (1989) in the Givetian of the Dinant Basin. Most of the bioclasts are micritized. Cross-bedding is present and has been significantly destroyed by bioturbation. Calcite microspar can be well developed transforming the packstone in a “false” grainstone. It is associated with pseudomorphs of larger acicular and square-off crystals. Rare key-vugs (DUNHAM, 1970; ESTEBAN & KLAPPA, 1983) occur in the thicker laminae.

Interpretation: algal shoal with accumulation of bioclasts from seagrass meadows (see microfacies 8) in the euphotic zone of a shallow subtidal environment. The environment is characterized by the same general energy dynamics as in previous microfacies.

Semi-restricted back-shoal environment with moderate energy

Microfacies type 8 (MF8) (Pl. 6, Figs 3-4)

Description: issinellid baffestone, peloidal packstone and “false” grainstone with kamaenids, triangulinellids, codiaceans (reworked *Bevocastria* and *Ortonella* nodules), molluscs, ostracods, *Bisphaera*, rare crinoids, brachiopods, trilobites and bryozoans, the latter occurring in millimetre-thick interlayered levels. Calcispheres are common as lumps containing well-preserved sponge spicules and small-sized bipyramidal quartz. The micritic matrix can be strongly microsparitized giving a homogeneous mosaic of greyish and whitish small-sized calcite crystals. Large saddle dolomite is associated with the microspar. This leads to the formation of “false” grainstones without different phases of cementation.

Interpretation: seagrass meadows in the euphotic zone of a shallow subtidal environment.

Microfacies type 9 (MF9) (Pl. 6, Figs 5-6)

Description: mudstone and wackestone with a few issinellids, kamaenids, *Bevocastria*, gastropods and ostracods with stacked carapaces. Irregular radial oolites (200 µm) are regularly observed. Small-sized bipyramidal quartz grains associated with codiacean lumps are present. Pyrite is common in the matrix. The micritic matrix is microsparitized and contains irregular mud-cracks and saddle dolomite. Relicts of anhydrite are exceptionally observed.

Interpretation: microflora and microfauna are drastically reduced and point to a very quiet semi-restricted environment. Salinity oscillations are indicated by the endemism of organisms, probable pseudomorphs after sulphate crystals precipitated from hypersaline brines. The algal and cyanobacterial associations indicate stressfull conditions. This microfacies is equivalent to the MF9 of PRÉAT & MAMET (1989) and is the most typical for the Givetian of the Dinant Basin in Belgium and France. Here, in the Terres d'Haur Fm, it is present but not well-represented, forming occasional levels at the transition from the Trois-Fontaines Fm to the Terres d'Haur Fm.

Restricted environments with salinity fluctuations

Microfacies type 10 (or MF10) (Pl. 6, Figs 7-8)

Description: mudstone with abundant ostracods, pelecypods, rare kamaenids and issinellids, and micritized oolites (200 -400 µm). The micritic matrix contains abundant thin vertical micro-fractures or probably sheet-cracks and large-sized subangular intraformational microbreccias with ostracod coquina levels and oolites. The microbreccias can form stratiform levels in the matrix. Anhydrite relicts, small pyrite (10 – 20 µm) and very fine-grained quartz (10 µm) are present. Fine crystalline idiopathic dolomite can partly replace the matrix.

Interpretation: very low diversity of organisms suggests significantly stressfull environment with possible emersion as indicated by the mud-cracks and *in situ* microbreccias. The sediments were subjected to hypersaline conditions as indicated by anhydritic relicts.

Reflux evaporitic brines (microfacies 5 – 8)

Relicts of anhydrite, squared-off crystal molds, isolated intraformational breccias and micro-cracks in the micritic matrix suggest the influence of former

evaporites in up-dip environments. The coarse-grained calcite microspar mainly observed in microfacies 5 to 8 could be a product of reflux hypersaline brines in the mid/inner ramp transition. A similar situation has been described in the Ordovician of Oklahoma by WAHLMAN (2010).

During the development of the Terres d'Haur Fm succession the sedimentation regime in the studied area was characterized by marine bioclastic and oolitic shoal/beach lagoonal subtidal-intertidal porous sands and muddy matrices. The brines that refluxed through these more down-dip ramp facies became somewhat depleted or less saturated and anhydritization proceeded. It replaced partly or totally the previous sediments and during later burial diagenesis calcite microspar replaced the sulfates as a “cement”. The sediment may become a “false” grainstone in the case of intensive replacement.

This has also been reported in the Visean of Northern France (MAMET & PRÉAT, 2005). Later on saddle dolomite may have replaced former calcite.

Sedimentary model

The Terres d'Haur Fm consists of an open marine shallow-water ramp facies. The outer ramp (microfacies 1) is characterized by deposition of argillaceous and silty carbonate muds from suspension. Only the most severe storms affected the seafloor and wave reworking is therefore exceptional. Mid-ramp deposits (microfacies 2 to 5) consist of various wackestones, packstones and grainstones, deposited below fair-weather wave base and reflecting varying degree of storm influence (intermediate and proximal tempestites), depending of the water depth and the depth of wave base. The general setting was quite shallow in the euphotic zone as indicated by the abundant green algae. Most of the bioclasts consist largely of autochthonous organisms, which have been reworked and sometimes embedded in cross-stratifications and tempestites. Inner-ramp deposits (microfacies 6 to 10) consist of oolitic or algal shoals and back-shoal sediments. The former are represented by laminar and cross-stratified packstones, grainstones, rudstones and bafflestones while the latter, i.e. the peritidal sediments, are mudstones and wackestones with semi-restricted biota. The shoals (oolites or palaeoberesellids – i.e. issinellids, kamaenids, triangulinellids) were probably small-sized, with low relief, since they did not constitute massive successions and are interlayered at a decimetre scale with fore- and back-shoals sediments. Similar palaeoberesellid shoals have been described in the Late

Dinantian of North Lancashire, England (HORBURY, 1992) and formed from the reworking palaeoberesellid buildups with heights between 1 and 2 metres. Small-sized coral-stromatopore patch reefs colonized the fore shoal areas near the top of our section. They did not seem to have taken a great development and were systematically destroyed forming floatstones and rudstones of microfacies 4 and 5.

Sequence stratigraphy

The lithological curve, derived from the microfacies standard sequence, records a shallowing-upward evolution of the sedimentation from subtidal to supratidal or littoral. The depositional pattern of an elementary parasequence or 5th-order sequence (*sensu* VAN WAGONER *et al.*, 1987) results in an upward-shoaling association of facies in which bedsets were deposited in progressively shallowing water. This parasequence is bounded by marine flooding surfaces highlighting an abrupt increase in water depth. Taking this key parameter into account, the flooding surface is represented in our standard sequence by a return

of microfacies 4 to 10 of the very shallow-water mid- and inner ramp to microfacies 1, 2 or 3, which are characterized by suspension of argillaceous and carbonate muds. As a consequence the subdivision of the lithological curve has been based on the successive occurrences of the three first microfacies along the section. This leads to the succession of 13 elementary parasequences (PSQ-1 to PSQ-13, Fig. 2) displaying variable thicknesses from decimetres to inframetres. Their stacking seems random, however two parasequence sets (4th-order, PSQS-A and PSQS-B, Fig. 2) can be distinguished. Each of them presents a thinning-upward of its parasequences, although more pronounced for PSQS-A, but both probably associated with a relative transgressive evolution. The elementary parasequences of PSQS-B have homogeneous thicknesses and are thicker than those of PSQS-A, suggesting an aggradation in a transgressive evolution. This relative sea-level increase superseded the lowstand systems tract of the underlying Trois-Fontaines Fm (MAMET & PRÉAT, 2005; CAMBIER, 2009; CASIER *et al.*, 2010) and suggests that the Terres d'Haur Fm represents a transgressive systems tract. During this evolution the lagoon of the

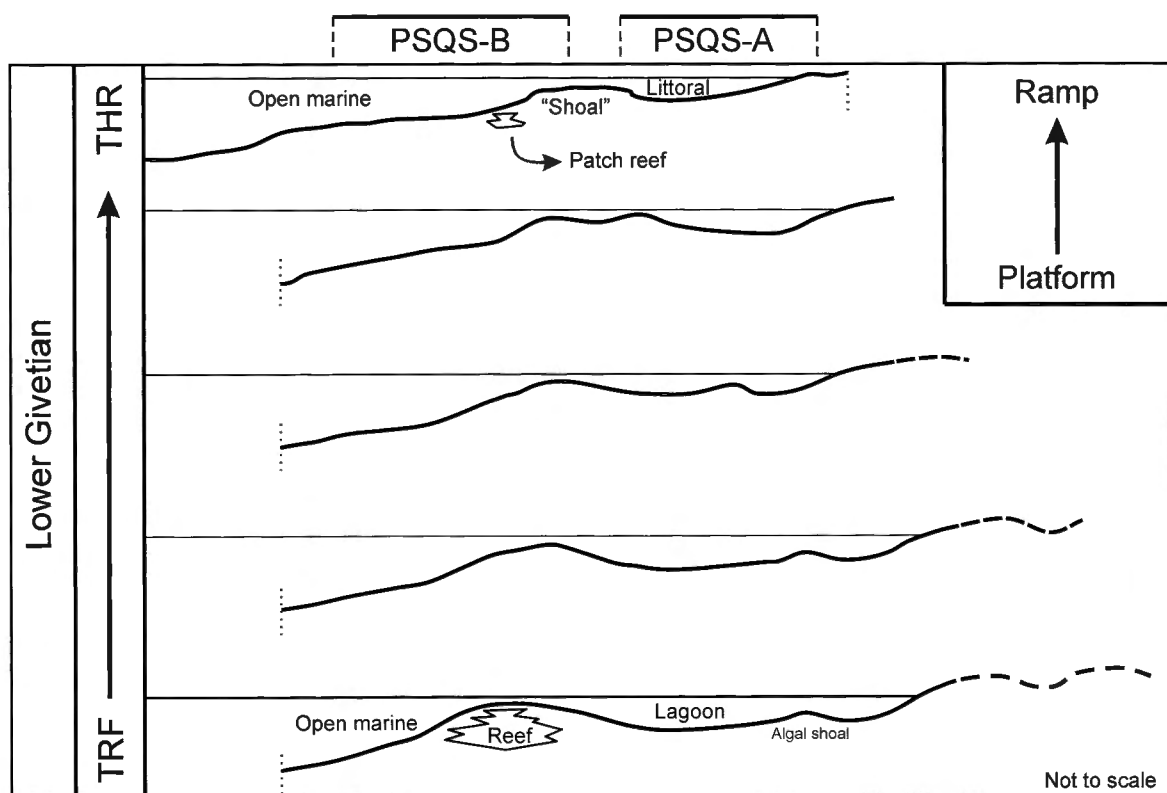


Fig. 4 – Progressive evolution of the restricted (lagoonal) carbonate platform (Trois-Fontaines Fm) to a ramp system (Terres d'Haur Fm). The former reefal barrier (PRÉAT & MAMET, 1989) is replaced by algal and oolitic shoals with occasional small patch reefs in the fore-shoal areas. PSQS-A and PSAQ-B are acronyms of parasequence set-A and parasequence set-B respectively (4th-order sequences) (see text).

Trois-Fontaines Fm has been progressively drowned (Fig. 4), as indicated by the microfacies and magnetic curve evolutions, and has been succeeded by the development of a coral-biostrome or “third biostrome” *sensu* PREAT & MAMET (1989). This stacking pattern of the elementary parasequences being random their correlation potential is weak. The open environment at the base of the elementary parasequences evolved to semi-restricted or littoral environments in the PSQS-A, and to shoals with strong reworking in the PSQS-B.

Magnetic susceptibility (X. DEVLEESCHOUWER & E. PETITCLERC)

The magnetic susceptibility (=MS) log measured in drillholes is a relatively old method of obtaining data about the nature and the content of magnetic minerals in rock series. MS logging of deep-sea rocks has become a routine procedure during Ocean Drilling Program (ODP) during the eighties (PONOMAREV & NEOCHOROSHKOV, 1984; BLOEMENDAL *et al.*, 1989). During the nineties, MS studies were applied to older rocks such as the Devonian carbonates of the Tafilalt and Mader basins (CRICK *et al.*, 1994) and the Upper Devonian (Frasnian-Famennian boundary) in Europe (DEVLEESCHOUWER, 1999; DEVLEESCHOUWER *et al.*, 1999). The changes in the flux of detrital material coming into the sedimentary environment represent an important cause of the MS variations (ELLWOOD *et al.*, 2000). These are related to the changes in the terrigenous clastic material supplied from the continent to the marine realm (CRICK *et al.*, 2001). It is generally explained by sea-level oscillations with high MS values during regressions where an increase of erosion on exposed continental masses can deliver more detrital minerals into the marine realm. On the contrary, low MS values are recorded during transgressive episodes (CRICK *et al.*, 1997, 2000, 2001). An increased detrital input to the marine domain will enhance the MS signal due to a higher abundance of grains of magnetic material. Different sources of non-carbonate (mostly terrigenous material) are related to riverine (CRICK *et al.*, 2000, 2001), volcanic activity (GORBARENKO *et al.*, 2002), hydrothermal vents (BORRADAILE & LAGROIX, 2000), bolide impacts (ELLWOOD *et al.*, 2003), eolian supply (HLADIL, 2002; HLADIL *et al.*, 2006) and products of pedogenesis during the formation of paleosols (CHEN *et al.*, 2005).

MS logging is considered to be a very useful high-resolution stratigraphic tool with great potential for correlations of sedimentary sequences within the same

basin or even between different basins (ELLWOOD *et al.*, 2001, 2007, 2008; RIQUIER *et al.*, 2010). The use of the MS logging for the Paleozoic sediments is meaningful only with a biostratigraphic control and the use of other techniques such as microfacies analysis.

Material and methods

In this study, the same samples used for sedimentological analyses were sliced into rectangular parallelepiped rock pieces. The MS measurements were carried out at the Royal Belgian Institute of Natural Sciences using MFK1-A susceptometer at room temperature in a low AC magnetic field of 400 A/m and at a frequency of 976 Hz. The MS values of the samples were corrected for the susceptibility of the empty plastic holder. Each sample was weighted with a precision of 0.01 g, measured three times and the results averaged. A mass specific low-field MS (X_{LF}) was calculated for each sample. The X_{LF} integrates the contribution of the different magnetic mineral fractions according to their dia-, para- or ferromagnetic *s.l.* behaviour. Any change in the composition, concentration and grain-size of the minerals is expressed in the X_{LF} value. In the sedimentary rocks, the MS curve records fluctuations in the amounts and contributions of diamagnetic (mostly quartz, calcite), paramagnetic (mostly clay minerals, pyrite and iron carbonates) or ferromagnetic *s.l.* phases (iron oxides and oxyhydroxides, iron-rich sulphides). Thus bed-by-bed X_{LF} logging through the section can display changes in the flux and/or sources of detrital input (ANDREWS & STRAVERS, 1993; ROBINSON, 1993; VANDERAVEROET *et al.*, 1999; ELLWOOD *et al.*, 2000).

Magnetic Susceptibility curve

The low-field MS values ranging between -2.093×10^{-9} and $1.94 \times 10^{-7} \text{ m}^3/\text{kg}$ (Fig. 2) are weak as usually observed in most of the carbonate rocks (between 1×10^{-9} and $1 \times 10^{-7} \text{ m}^3/\text{kg}$; ELLWOOD *et al.*, 1999). The highest X_{LF} value ($1.94 \times 10^{-7} \text{ m}^3/\text{kg}$) was measured in MF8 corresponding to a restricted back-shoal environment of the Terres d'Haur Fm. Despite the low X_{LF} values, the MS signal varies along the lithological column with several MS evolutions (MSE) reported as magnetic sequences. Eight MSE, numbered MSE 1 to MSE 8, were identified (Fig. 2) and are subdivided into short-term MSE by alphabetical letters. MSE 1, beginning at the base of the section in the Terres d'Haur Fm, displays large MS fluctuations superimposed on a main increasing X_{LF} trend from 0.665 to $1.94 \times 10^{-7} \text{ m}^3/\text{kg}$. This first magnetic sequence can be correlated

partly to the regressive evolution from a mid-ramp under the influence of storms (MF3) to the back-shoal environment within the fair-weather wave zone (MF9). MSE 2 records a decreasing X_{LF} trend interrupted at the top by higher values (MSE 2C). This evolution is more or less similar with the microfacies curve. MSE 3A shows a long decreasing evolution of the X_{LF} values mirrored in the microfacies curve, which records a transgressive evolution from restricted environment close to the emersion in hypersaline conditions (MF10) to the open-marine environment influenced by storm activities (MF3). MSE 3B, characterised by

a gradual increase of the X_{LF} values, corresponds to the development of the oolitic shoal. The next four MSE (MSE 4-7) shows numerous smaller-scale fluctuations of the X_{LF} values mostly comprised between 0.65 and $1.4 \times 10^{-7} \text{ m}^3/\text{kg}$. Finally, MSE 8 shows a significant decreasing trend of the X_{LF} values (from $1.59 \times 10^{-7} \text{ m}^3/\text{kg}$) observed across the boundary between the Terres d'Haurs and the Mont d'Haurs Fm. The latter evolution is characterised by the lowest, sometimes negative, X_{LF} values of the section. It is important to notice that the X_{LF} trend in MSE 8 and the microfacies curve are opposite.

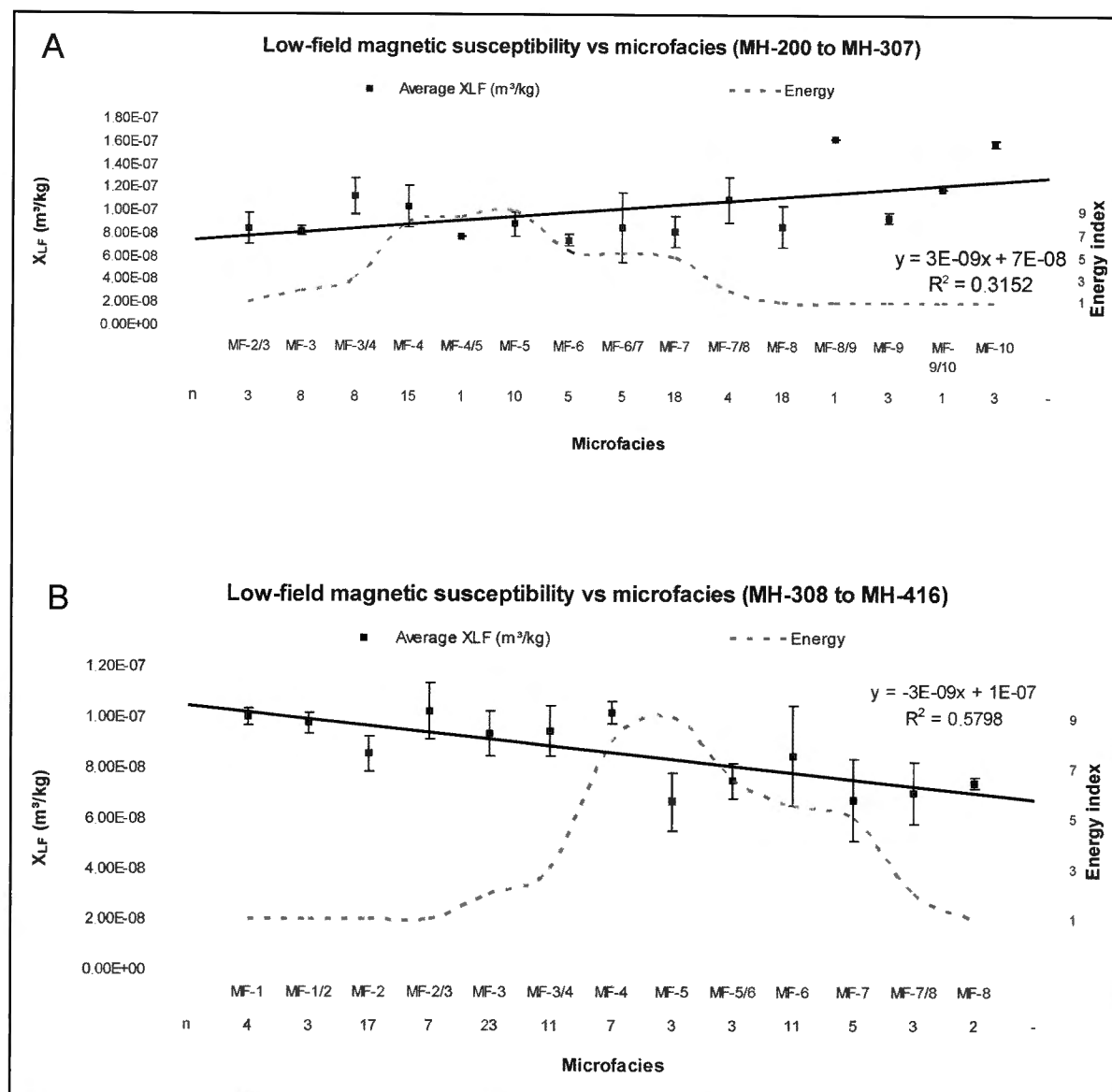


Fig. 5 – The mean low-field MS values plotted against microfacies in the Mont d'Haurs section. The coefficient of determination is assigned to each model. A) Linear regression line and model for the lower half of the section (samples MH200-MH307), B) Linear regression line and model for the upper part of the Terres d'Haurs Fm (samples MH308 – MH416).

Comparison between microfacies and X_{LF} curves

The evolutions of the X_{LF} and microfacies curves show mimetic evolutions during the lower half of the section (samples MH 200 to MH 307). Opposite evolutions are observed in the X_{LF} and microfacies curves for the upper part of the Terres d'Haur Fm (samples MH 308 to MH 416). These observations suggest reporting the data into two different models based on these samples (Fig. 4). The mean X_{LF} values with their standard deviations are plotted against microfacies and the number of samples (n) in each microfacies is indicated for both models (Figs 5A and 5B).

The first model has a linear regression (black line, Fig. 5A) characterised by a coefficient of determination $R^2 = 0.31$ (indicating that 31 % of the variability in the data is explained by this model). The correlation coefficient $r = 0.56$ indicates a moderately positive correlation between these two parameters. The average X_{LF} value slightly fluctuates between $8.22 \times 10^{-8} \text{ m}^3/\text{kg}$ for microfacies MF2-3 in the open-marine environment to $8.45 \times 10^{-8} \text{ m}^3/\text{kg}$ for microfacies MF8 (semi-restricted environment). In restricted environment (microfacies MF10), average X_{LF} values fluctuate and increase up to $1.59 \times 10^{-7} \text{ m}^3/\text{kg}$. The energy index indicating the water agitation is also reported for each microfacies on a scale ranging from 1 (low energy like in the outer and mid-ramp under the temporary influence of storms) to 9 (highest energy associated to the oolitic and algal shoals in the inner ramp). The average X_{LF} values decrease slightly in the more energetic environments of the mid- and inner ramp and are the highest in the semi-restricted to restricted conditions close to the continent.

The second model is characterised by a linear regression (black line, Fig. 5B) with a coefficient of determination $R^2 = 0.58$ (indicating that 58 % of the variability in the data is explained by this model). The correlation coefficient $r = -0.76$ indicates a moderately strong negative correlation between these two parameters. The microfacies reported in the second model vary from open marine environment in the outer ramp (MF1) to semi-restricted environment (MF8). The average X_{LF} values fluctuate slightly between the outer ramp (MF1) and the mid-ramp (MF4) ranging between 0.8 and $1.0 \times 10^{-7} \text{ m}^3/\text{kg}$. The average X_{LF} values decrease in the microfacies (MF5) and fluctuate slightly from the open marine fore-shoal to back-shoal environment (MF8) ranging between 0.66 and $0.85 \times 10^{-7} \text{ m}^3/\text{kg}$. The energy index indicating the water agitation is reported for each microfacies and ranges from 1 (low energy) to 9 (highest energy). The average

X_{LF} values decrease slightly in the more energetic environments of the mid- and inner ramp but are the highest for the microfacies in the outer and mid-ramp under the influence of storms.

These models established for the Terres d'Haur Fm indicate the transitional phase from a carbonate rimmed-shelf of the Trois-Fontaines Fm to the carbonate ramp of the Terres d'Haur Fm as indicated by the progressive disparition of the reefal barrier at the end of the Trois-Fontaines Fm and the base of the Terres d'Haur Fm (CASIER *et al.*, 2010). The first model (Fig. 5A) proposed here show moderate positive correlation between the microfacies and the X_{LF} values suggesting a carbonate platform profile such as those proposed for the Frasnian (DA SILVA *et al.*, 2009) or the Givetian in the Trois-Fontaines Fm (CASIER *et al.*, 2011) and the Fromelles Fm (DEVLEESCHOUWER *et al.*, 2010). The second model (Fig. 5B) records the carbonate ramp morphology confirmed by the negative strong correlation coefficient between microfacies and X_{LF} values. This model is quite different from the mixed siliciclastic-carbonate ramp profile observed in the Hanonet Fm of the "La Couvinoise" section in Belgium (DA SILVA *et al.*, 2009).

Comparison with MS data from other sections

A paleoenvironmental model, corresponding to a ramp profile, is proposed for the Terres d'Haur Fm in the "Les Monts de Baileux section". In this section, the Terres d'Haur Fm is 60 metres thick, subdivided into 5 lithological units, and overlain by 15 metres of metre-thick biostromal beds and thinner slightly argillaceous limestones belonging to the Mont d'Haur Fm (MABILLE & BOULVAIN, 2008). The mean MS values decrease from the outer ($6.48 \times 10^{-8} \text{ m}^3/\text{kg}$) to inner ($7.98 \times 10^{-8} \text{ m}^3/\text{kg}$) ramp along the profile, with lower MS values in more energetic environments (ooloidal shoal: $6.09 \times 10^{-8} \text{ m}^3/\text{kg}$). Their range is quite similar with the average X_{LF} values observed in the Mont d'Haur section. Based on the sedimentary environments and the sequential analysis, only the lower part of the Terres d'Haur Fm (Fig. 5A) presents similar MS data along the ramp profile, whereas an inverse relation is observed for the upper part of the Terres d'Haur Fm defined here in the stratotype area. The average X_{LF} values in the upper part of the Terres d'Haur Fm are more homogeneous compared to those reported in the lower half of the Terres d'Haur Fm. The MS curve produced for the "Les Monts de Baileux" section, even with a lower resolution of samples, shows a stable phase of MS values at the base of the Terres d'Haur Fm followed

by two successive decreasing trends with the lowest MS values observed at the base of the Mont d'Haur Fm. In the stratotype area, the MS signal decreases also across the boundary between the Terres d'Haur and Mont d'Haur Fm (MSE 8) and three smaller MS peaks are observed in both sections at the base of the Mont d'Haur Fm. These MS data can serve as high-resolution stratigraphic correlation markers for the base of the Mont d'Haur Fm in Belgium and France, in sections 40 km apart.

Ostracods (J.-G. CASIER & J. MOREAU)

Previous studies at the Mont d'Haur

Ostracods collected in the Terres d'Haur Fm and in the Mont d'Haur Fm at the Mont d'Haur have been studied by COEN (1985). A list of specimens figured by COEN, and recently included in the collection of the Department of Paleontology at the Royal Belgian Institute of Natural Sciences, is reported in CASIER *et al.* (2011).

The ostracods described by COEN (1985) from the Terres d'Haur Fm were extracted from a sample collected just above a hiatus corresponding to the entry of a subway in the fortification, which probably correspond to the upper part of the Terres d'Haur Fm, outcropping in section 4.

BECKER & BLESS (1974) mentioned and figured *Coryellina* sp. G MAGNE, 1964, and *Samarella* cf. *crassa* POLENOVA, 1952, in the Terres d'Haur Fm at the Mont d'Haur without further informations. Finally, CASIER (*in CASIER et al.*, 2010) reported a series of species in the base of the Terres d'Haur Fm outcropping in the Rancennes Quarry (Fig. 1, section 2) at the Mont d'Haur.

Material and methods

Forty-eight samples of approximately 500 g each were collected in sections 3 and 4 (Fig. 1). All samples were crushed by a hydraulic press and approximately 100 g of each sample was processed using 99.8% glacial acetic acid, at nearly 90°C, for four days at a rate of eight hours a day. This mode of extraction, called the hot acetolysis method, was described by LETHIERS & CRASQUIN-SOLEAU (1988). The residues were sieved on 250 µm and 1600 µm mesh screens. The process was repeated two times, and approximately 4,660 carapaces, valves and fragments of ostracods identifiable at any taxonomic level were thus extracted.

In two samples ostracods were absent (MH-203, 211) and in five other samples, ostracods were rare, poorly preserved, and consequently unidentifiable (MH-205, 209, 214, 275, 337). In 21 samples the number of ostracods was lower than 10 per 10 g sorted; in 7 samples the abundance varies from 10 up to 20 specimens; in 9 samples, from 20 up to 50; in 5 samples, from 50 up to 100. Four samples contained more than 100 ostracods per 10 g sorted: MH-201 (133), MH-243 (210), MH-298 (430), MH-332 (104). Fifty-two ostracod species have been identified in the two studied sections. Their stratigraphic positions, distribution and the number of ostracod species per sample are shown in Fig. 2 and Table 2.

Systematic position of the ostracod taxa

ORDER LEPERDITICOPIDA SCOTT, 1961
Leperditicopida? indet.

ORDER PALAEOCOPIDA HENNINGSMOEN, 1953
Suborder Palaeocopina HENNINGSMOEN, 1953

Superfamily Kirkbyoidea ULRICH & BASSLER, 1906
Family Amphissitidae KNIGHT, 1928
Amphissites tener BECKER, 1964
Pl. 1, Fig. 1

Superfamily Hollinoidea SWARTZ, 1936
Family Hollinidae SWARTZ, 1936
Parabolbinella coeni CASIER, 2011
Pl. 1, Fig. 2

Hollinidae gen. & sp. indet. 1
Pl. 1, Fig. 14

Family Ctenoloculinidae JAANUSSEN & MARTINSSON, 1956
Ctenoloculina sp. A, aff. *kelletae* POKORNY, 1950
Pl. 1, Fig. 3

Superfamily Beyrichioidea MATTHEW, 1886
Family Beyrichiidae MATTHEW, 1886
Kozlowskiella? *rugulosa* (KUMMEROW, 1953)
Pl. 1, Fig. 4

Kozlowskiella sp. A *sensu* BECKER, 1964
Pl. 1, Fig. 6

“*Kozlowskiella*” sp. B
Pl. 1, Fig. 7

Kozlowskiella sp. C
Pl. 1, Fig. 5

- Superfamily Aparchitoidea JONES, 1901
 Family Aparchitidae JONES, 1901
 "Aparchites" sp. indet.
 Pl. 1, Fig. 12
- Superfamily Primitiopoidea SWARTZ, 1936
 Family Primitiopsidae SWARTZ, 1936
Parapribylites hanaicus POKORNY, 1950
 Pl. 1, Fig. 8
- Coryellina curta* POLENOVA in ROZHDESTVENSKAJA, 1959
- Kielciella fastigans* (BECKER, 1964)
 Pl. 1, Fig. 9
- Kielciella* cf. *arduennensis* ADAMCZAK & COEN, 1992
 Pl. 1, Fig. 10
- ?Family Buregiidae POLENOVA, 1953
Buregia ovata (KUMMEROW, 1953)
 Pl. 1, Fig. 13
- Superfamily Kirkbyoidea ULRICH & BASSLER, 1906 ?
 Family Scrobiculidae POSNER, 1951
Roundyella patagiata (BECKER, 1964)
 Pl. 1, Fig. 11
- Suborder Paraparchitocopina
 GRAMM in GRAMM & IVANOV (1975)
- Superfamily Paraparchitoidea SCOTT, 1959
 Family Paraparchitidae SCOTT, 1959
Coeloenellina minima (KUMMEROW, 1953)
 Pl. 1, Fig. 15
- Coeloenellina vellicata* COEN, 1985
 Pl. 2, Fig. 1
- Suborder Platycopina SARS, 1866
 Superfamily Kloedenelloidea ULRICH & BASSLER, 1908
 Family Kloedenellidae ULRICH & BASSLER, 1908
Samarella n. sp., aff. *laevinodosa*
 POLENOVA, 1952 sensu CASIER & PRÉAT, 1991
 Pl. 2, Fig. 2
- Samarella?* sp. A
 Pl. 2, Fig. 3
- Poloniella tertia* KRÖMMELBEIN, 1953
 Pl. 2, Fig. 4
- Poloniella claviformis* (KUMMEROW, 1953)
 Pl. 2, Fig. 5
- Uchtovia abundans* (POKORNY, 1950)
 Pl. 2, Fig. 7
- Uchtovia refrathensis* (KRÖMMELBEIN, 1954)
 Pl. 2, Fig. 8
- Evlanelia germanica* BECKER, 1964
 Pl. 2, Fig. 9
- Evlanelia mitis* ADAMCZAK, 1968
 Pl. 2, Fig. 10
- Evlanelia* cf. *lessensis* CASIER, 1991
 Pl. 2, Fig. 11
- Family Beyrichiopsidae HENNINGSMOEN, 1953
Marginia sculpta multicostata POLENOVA, 1952
 Pl. 2, Fig. 6
- Superfamily Cytherelloidea SARS, 1866
 Family Cavellinidae EGOROV, 1950
Cavellina devoniana EGOROV, 1950
 Pl. 2, Fig. 12
- Cavellina* cf. *rhenana* KRÖMMELBEIN, 1954
 Pl. 2, Fig. 13
- ORDER PODOCOPIDA SARS, 1866
 Suborder Metacopina SYLVESTER-BRADLEY, 1961
 Superfamily Healdoidea HARLTON, 1933
 Family Healdiidae HARLTON, 1933
Cytherellina obliqua (KUMMEROW, 1953)
 Pl. 3, Fig. 2
- Cytherellina* sp. A, aff. *obliqua* (KUMMEROW, 1953)
 Pl. 3, Fig. 1
- Cytherellina* sp. B, aff. *obliqua* (KUMMEROW, 1953)
 Pl. 3, Fig. 3
- Cytherellina* sp. A sensu CASIER, 2011
- Cytherellina perlonga* (KUMMEROW, 1953)
 Pl. 3, Fig. 4
- Superfamily Thlipsuroidea ULRICH, 1894
 Family Thlipsuridae ULRICH, 1894
Polyzygia symmetrica GÜRICH, 1896
 Pl. 3, Fig. 8
- Superfamily Quasillitoidea CORYELL & MALKIN 1936
 Family Quasillitidae CORYELL & MALKIN, 1936
Quasillites fromelennensis MILHAU, 1983
 Pl. 3, Fig. 7
- Jenningsina heddebauti* MILHAU, 1983
 Pl. 3, Fig. 5
- Jefina romei* COEN, 1985?
 Pl. 3, Fig. 6

SECTIONS 3 AND 4	201	204	216	221	227	233	238	239	243	249	255	261	267	282	289	298	305	309	319	332
<i>Cytherellina</i> sp. B, aff. <i>obliqua</i> (KUMMEROW, 1953)	*																			
<i>Jefina romei</i> COEN, 1985	?																			
<i>Bairdia</i> cf. <i>paffrathensis</i> KUMMEROW, 1953	*																			
<i>Cytherellina</i> sp. A sensu CASIER 2011	*			*																
<i>Evlanella germanica</i> BECKER, 1964	*				*	*	*	?												
" <i>Healdianella</i> " <i>budensis</i> OLEMPSKA, 1979	*	*														*	?			
<i>Marginia sculpta multicostata</i> POLENOVA, 1953	?	*																		
<i>Buregia ovata</i> (KUMMEROW, 1953)	*	*			*	*	*	*				*							*	
<i>Polyzygia symmetrica</i> GÜRICH, 1896	*																			
<i>Quasillites fromelennensis</i> MILHAU, 1983	*				*	*	*	*	*	*	*	*	*	*	*	*	*	*	*	
<i>Jenningsina heddebauti</i> MILHAU, 1983	*	?				?	?													*
<i>Poloniella tertia</i> KRÖMMELBEIN, 1953	*			*		?														*
<i>Cytherellina obliqua</i> (KUMMEROW, 1953)	*	*		*	*	*	*													*
<i>Cytherellina perlonga</i> (KUMMEROW, 1953)	*																			*
<i>Bairdia paffrathensis</i> KUMMEROW, 1953	*	*	*		*	*	*													
<i>Cavellina devoniana</i> EGOROV, 1950		*			*	*	*													
<i>Uchtovia abundans</i> (POKORNY, 1950)	?				*											?	*	*	*	
Hollinidae sp. indet. 1			*																	
Leperditicopida indet.			?																	
<i>Kozlowskiella?</i> <i>rugulosa</i> (KUMMEROW, 1953)		*													*	*				
<i>Amphissites tener</i> BECKER, 1964			?	*		?									*	*				
<i>Kielciella</i> cf. <i>arduennensis</i> ADAMCZ. & COEN, 1992				?																*
<i>Cavellina</i> cf. <i>rhenana</i> KRÖMMELBEIN, 1954					*										*					
<i>Evlanella</i> sp. indet.					*										*	*				
<i>Evlanella mitis</i> ADAMCZAK, 1968					*	?		?												
<i>Cytherellina</i> sp. A, aff. <i>obliqua</i> (KUMMEROW, 1953)					*	*														*
<i>Uchtovia refrathensis</i> (KRÖMMELBEIN, 1954)					?										?	?	?			
<i>Parapribylites hanaicus</i> POKORNY, 1950						*	*	*	*	*					?	*	*	*	*	*
" <i>Kozlowskiella</i> " sp. B						*														*
<i>Coeloenellina minima</i> (KUMMEROW, 1953)						*	*		?								*	*		
<i>Poloniella claviformis</i> (KUMMEROW, 1953)						*	?	*	*								*	*	*	*
<i>Kozlowskiella</i> sp. A sensu BECKER, 1964							?	*									*			
<i>Kielciella fastigans</i> (BECKER, 1964)															*					
Palaeocopina indet.															*					
" <i>Orthocypris</i> " sp. indet.															*	*	*	*	*	
<i>Coeloenellina vellicata</i> COEN, 1985															*					
<i>Parabolbinella coeni</i> CASIER, 2011															*					
<i>Ropolonellus kettneri</i> (POKORNY, 1950)															?					
<i>Coryllina curta</i> POLENOVA (in ROZH., 1959)															?					
<i>Bairdiacypris antiqua</i> (POKORNY, 1950)																*				
<i>Ctenoloculina</i> sp. A, aff. <i>kelletae</i> POKORNY, 1950																*				
<i>Microcheilinella affinis</i> POLENOVA, 1955?																*				
<i>Tubulibairdia clava</i> (KEGEL, 1932)																*				
<i>Kozlowskiella</i> sp. C																				*
<i>Bairdia</i> cf. <i>tischendorfi</i> BECKER, 1965																				*
<i>Orthocypris cicatricosa</i> COEN, 1985																				*
<i>Acratia lucea</i> MAILLET, 2010, nom. nud.																				*
<i>Bairdia</i> sp. indet.																				
<i>Bufina schaderthalensis</i> ZAGORA, 1968																				
<i>Samarella</i> n. sp., aff. <i>laevinodosa</i> POL., 1952																				
<i>Bairdiocypris rauffi</i> KRÖMMELBEIN, 1952																				
<i>Zeuschnerina dispar</i> ADAMCZAK, 1976																				
<i>Samarella?</i> sp. A																				
<i>Microcheilinella</i> sp. indet.																				
<i>Roundyella patagiata</i> (BECKER, 1964)																				
<i>Aparchites</i> sp. indet.																				

Table 2 – Distribution of ostracods in the Terres d'Haurs Fm and in the base of the Mont d'Haurs Fm

	333	341	345	354	360	369	377	384	391	400	404	408	413	417	419	422	424	429	431	436	SECTIONS 3 AND 4	
																					Cyperellina sp. B, aff. obliqua (KUMMEROW, 1953)	
	*																				Jefina romei COEN, 1985	
																					Bairdia cf. paffrathensis KUMMEROW, 1953	
																					Cyperellina sp. A sensu CASIER 2011	
																					Evlanella germanica BECKER, 1964	
																					"Healdianella" budensis OLEMPSKA, 1979	
																					Marginia sculpta multicostata POLENOVA, 1953	
																					Buregia ovata (KUMMEROW, 1953)	
																					Polyzygia symmetrica GÜRICH, 1896	
																					Quasillites fromelennensis MILHAU, 1983	
																					Jenningsina heddebauti MILHAU, 1983	
																					Poloniella tertia KRÖMMELBEIN, 1953	
																					Cyperellina obliqua (KUMMEROW, 1953)	
																					Cyperellina perlonga (KUMMEROW, 1953)	
																					Bairdia paffrathensis KUMMEROW, 1953	
																					Cavellina devoniana EGOROV, 1950	
																					Uchtovia abundans (POKORNY, 1950)	
																					Hollinidae sp. indet. 1	
																					Leperditicopida indet.	
																					Kozlowskiella? rugulosa (KUMMEROW, 1953)	
																					Amphissites tener BECKER, 1964	
																					Kielciella cf. arduennensis ADAMCZ. & COEN, 1992	
																					Cavellina cf. rhenana KRÖMMELBEIN, 1954	
																					Evlanella sp. indet.	
																					Evlanella mitis ADAMCZAK, 1968	
																					Cyperellina sp. A, aff. obliqua (KUMMEROW, 1953)	
																					Uchtovia refrathensis (KRÖMMELBEIN, 1954)	
																					Parapribylites hanaicus POKORNY, 1950	
																					"Kozlowskiella" sp. B	
																					Coeloenellina minima (KUMMEROW, 1953)	
																					Poloniella claviformis (KUMMEROW, 1953)	
																					Kozlowskiella sp. A sensu BECKER, 1964	
																					Kielciella fastigans (BECKER, 1964)	
																					Palaeocopina indet.	
																					"Orthocypris" sp. indet.	
																					Coeloenellina vellicata COEN, 1985	
																					Parabolbinella coeni CASIER, 2011	
																					Ropolonellus kettneri (POKORNY, 1950)	
																					Coryellina curta POLENOVA (in ROZH., 1959)	
																					Bairdiacypris antiqua (POKORNY, 1950)	
				*																	Ctenoloculina sp. A, aff. kelletae POKORNY, 1950	
																					Microcheilinella affinis POLENOVA, 1955?	
																					Tubulibairdia clava (KEGEL, 1932)	
																					Kozlowskiella sp. C	
																					Bairdia cf. tischendorfi BECKER, 1965	
																					Orthocypris cicatricosa COEN, 1985	
						*															Acratia lucea MAILLET, 2010, nom. nud.	
							*														Bairdia sp. indet.	
								*													Bufina schaderthalensis ZAGORA, 1968	
									*												Samarella n. sp., aff. laevinodosa POL., 1952	
										*											Bairdiocypris rauffi KRÖMMELBEIN, 1952	
											*										Zeuschnerina dispar ADAMCZAK, 1976	
												*									Samarella? sp. A	
													*								Microcheilinella sp. indet.	
														*							Roundyella patagiata (BECKER, 1964)	
															*						Aparchites sp. indet.	

exposed in the sections numbered 3 and 4 on Fig. 1. The boundary is between samples MH-417 and MH-419.

Family Bufinidae SOHN & STOVER, 1961

Buferina schaderthalensis ZAGORA, 1968

Pl. 2, Fig. 14.

Family Ropolonellidae CORYELL & MALKIN, 1936

Ropolonellus kettneri (POKORNÝ, 1950)

Pl. 2, Fig. 15

Zeuschnerina dispar ADAMZCAK, 1976

Pl. 3, Fig. 9

Suborder Podocopina SARS, 1866

Superfamily Bairdiocypridoidea SHAVER, 1961

Family Bairdiocyprididae SHAVER, 1961

'Healdianella' budensis OLEMPSKA, 1979

Pl. 3, Fig. 12

Bairdiocypris rauffi KRÖMMELBEIN, 1952

Pl. 3, Fig. 10

Family Bairdiocyprididae SHAVER, 1961?

Orthocypris cicatricosa COEN, 1985

Pl. 3, Fig. 13

"*Orthocypris*" sp. indet. 1, 2

Pl. 3, Figs 14, 15

Family Pachydomellidae BERDAN & SOHN, 1961

Microcheilinella affinis POLENOVA, 1955

Tubilibairdia clava (KEGEL, 1932)

Pl. 3, Fig. 16

Superfamily Bairdioidea SARS, 1888

Family Acratiidae GRÜNDL, 1962

Acratia lucea MAILLET, 2010 nom. nud.

Pl. 3, Fig. 11

Family Bairdiidae SARS, 1888

Bairdia paffrathensis KUMMEROW, 1953

Pl. 3, Fig. 18

Bairdia cf. *paffrathensis* KUMMEROW, 1953

Pl. 3, Fig. 17

Bairdia cf. *tischendorfi* BECKER, 1965

Bairdiacypris antiqua (POKORNÝ, 1950)

Paleoecology of ostracods

Fifty-two ostracod species have been identified in the Terres d'Haur Fm and in the very base of the Mont d'Haur Fm at the Mont d'Haur, 14 belong to the Palaeocopina, two to the Paraparchiticopina, 12

to the Platycopina, 12 to the Metacopina, 11 to the Podocopina, and a fragment is assigned with doubt to the Leperditicopida. All species pertain to the Eifelian Mega-Assemblage, which corresponds to the incorrect term "Eifelian ecotype" of BECKER (*in* BANDEL & BECKER, 1975; see CASIER, 2004). Several neritic assemblages are recognized within this mega-assemblage, which are indicative of lagoonal (Ass. 0), semi-restricted (Ass. I) or marine environments from shallow waters, above fair-weather wave base (Ass. II) to deeper waters (Ass. III), below storm wave base (CASIER, 1987; see also CASIER, 2008, fig. 1; CASIER & PRÉAT, 2003, fig. 3). In this last assemblage, the relative proportion of metacopids and podocopids is related to the oxygen content of the bottom waters and consequently to the water depth. In deep neritic settings, only metacopid and palaeocopid ostracods are present, and in such a case the Ass. III corresponds to the Malvinokaffric "ecotype" of LETHIERS *et al.* (2001), as demonstrated by the recent study of ostracods from the Belen Fm at Pisacavina, in Bolivia (CASIER & RACHEBOEUF, 2008).

The ostracods in the base of the Terres d'Haur Fm, exposed in the Rancennes Quarry (Fig. 1, section 2), are indicative of semi-restricted or shallow marine environments under fair-weather wave base (CASIER *et al.*, 2010). The study of ostracods occurring in sections 3 and 4 shows that these shallow marine environmental conditions subsisted in the base of the Terres d'Haur Fm. In these two sections, the associations of ostracods are generally very diverse with numerous species belonging to the Palaeocopina, Platycopina, Metacopina and Podocopina proving that the living conditions were particularly favourable for these crustaceans. The occurrence of Podocopina is indicative of well-oxygenated water conditions, and of normal salinity or very close to normal values. The occurrence of many palaeocop and metacop species is indicative of calm environments below fair-weather wave base and commonly below storm wave base. The richness of ostracod fragments in numerous samples, particularly from MH-203 to MH-238, indicates the proximity of agitated marine waters. The occurrence of some stacked ostracod valves in several other samples (MH-233, 239, 298, 332, 400, and also observed in the MH-353 thin section), due to lapping, and the abundance of Platycopina and Paraparchiticopina are also indicative of very shallow settings. Monospecific assemblages indicative of semi-restricted water conditions occurred also in numerous samples, including the genera *Cytherellina* (MH-201, 233, 400), *Quasillites* (MH-243, 267, 289, 298), *Cavellina* (MH-360, 369) and

Parapribylites (MH-243, 249). Noteworthy, stacked ostracods due to lapping are generally present in samples characterized by monospecificity (GUERNET & LETHIERS, 1989). In reality it is the case for four out of six samples.

In the base of the Mont d'Haur Fm, ostracods are also abundant and diversified. The abundance of podocopids in all the samples indicates the persistence of well-oxygenated water conditions in shallow settings. The predominance of thick *Bairdia*, *Tubulibairdia* and *Bairdiocypris* in several samples (MH-422, 424, 429) is also indicative of stronger agitated water conditions. The abundance of ostracod fragments in sample MH-436 also points to the proximity of such environments.

Comparisons with ostracods previously identified at the Mont d'Haur or in other sections

The majority of the 26 ostracod species identified in the upper part of the Terres d'Haur Fm at the Mont d'Haur by COEN (1985) have been recorded in the present study, with the exception of *Refrathella struvei?*, *Balantoides brauni*, *Cytherellina groosae*, *Cryptophyllus* sp., and rarely represented or doubtful species belonging to the genera *Terasacculus*, *Aechmina* and *Leptoprimitia*. *Roponellus* cf. *aznajevaensis* (ROZHDESTVENSKAJA, 1962) in COEN (1985) corresponds to our *R. kettneri* (POKORNY, 1950).

A large number of species present at the Mont d'Haur are known in the Dinant Synclinorium, from Resteigne (CASIER & PRÉAT, 1990, 1991) and Glageon (CASIER et al., 1995), and in the Namur Synclinorium, from Aisemont (CASIER & PRÉAT, 2006). Close relationship exists also with the Boulonnais (MAGNE, 1964; MILHAU, 1983) and especially with Germany (KEGEL, 1932; KRÖMMELBEIN, 1952, 1953; KUMMEROW, 1953; BECKER, 1964, 1965; GROOS, 1969; ZAGORA, 1968). Several species are in common with Poland (ADAMCZAK, 1968, 1976; OLEMPSKA, 1979; ZBIKOWSKA, 1983), the Czech Republic (POKORNY, 1950), and the Russian platform (POLENOVA, 1955; ROZHDESTVENSKAJA, 1959, 1962). The relations with the Montagne Noire (Southern France) and the Maghreb (Algeria and Morocco) are on the contrary reduced (CASIER, 1985; CASIER et al., 1997, 2010), probably because the environments in these regions, except for the northwestern Meseta of Morocco (CASIER et al., 1997), were substantially deeper.

Conclusions

Ostracods in the Terres d'Haur Fm and in the base of the Mont d'Haur Fm at the Mont d'Haur are generally much diversified and belong exclusively to the Eifelian Mega-Assemblage. Fifty-two species have been identified which are generally indicative of marine environments below fair-weather wave base or below storm wave base. But, the relative abundance of Podocopina and Metacopina proves that environments were never very deep. Ostracods are sometimes indicative of semi-restricted environments, especially in the base of the Terres d'Haur Fm, but the sedimentological analysis shows that these ostracods have been mainly transported from these shallow settings. In the base of the Mont d'Haur Fm, thick-shelled ostracods indicate that the energy of the environment became stronger. The faunal change close to the boundary of the Terres d'Haur Fm and the Mont d'Haur Fm corresponds to an important shift of the low-field MS, and is probably related to the cessation of the influx of sediments from shallow settings.

Ten microfacies have been defined, encompassing open marine to supratidal environments with offshore channels and various shoals on a ramp setting. Three microfacies (one included in the external ramp, two in the mid-ramp) are situated below or near storm wave base. The next two microfacies (mid-ramp) are below the fair-weather wave base and are characterized by abundant organisms. The last microfacies belong to the inner ramp and include oolitic shoals and algal shoals, indicative of the euphotic zone. Most of microfacies are witnesses of storm deposits and some of them suffered diagenesis from probable reflux of evaporitic brines. The oolitic and algal shoals, developed behind several patch-reefs, characterize most of the lower part of the formation. Contrastingly, its upper part is marked by more open marine environments. The sequence stratigraphic analysis has led to the identification of two parasequence sets (PSQS-A and PSQS-B) that could be part of a TST (transgressive systems tract), characterising the whole Terres d'Haur Fm. The magnetic susceptibility describes a double evolution of the ramp characterized by the transition from a true platform system in the Trois-Fontaines Fm to a homoclinal ramp in the Terres d'Haur Fm.

The low-field MS values are weak and vary along the lithological column, allowing eight magnetic sequences to be identified. The MSE and the microfacies curve in the lower half of the section are more or less mimetic. MSE 3B characterised by a gradual increase of the X_{LF} values corresponds to the development of oolitic shoal.

The next four MSE show numerous smaller-scale fluctuations of the X_{LF} values, which seem inversely reported in the microfacies curve. Finally, MSE 8 shows a significant decreasing trend of the X_{LF} values across the boundary of the Terres d'Hauris and the Mont d'Hauris Fm towards the lowest, sometimes negative, X_{LF} values of the section.

Two linear regression models are presented and allow confirming: (1) a moderately positive correlation between X_{LF} values and microfacies in the lower half of the section and (2) a moderately strong negative correlation between these two parameters in the upper part of the Terres d'Hauris Fm and base of the Mont d'Hauris Fm. The water agitation is the highest in the mid- and inner ramp associated with the oolite and algal shoal environments and corresponds to the lowest average X_{LF} values in the section. The model established for the lower half of the section corresponds more to a carbonate platform profile in opposition to the second model, which records the carbonate ramp morphology.

The average X_{LF} values in the upper part of the Terres d'Hauris Fm are more homogeneous compared to those reported in the lower half of the Terres d'Hauris Fm. High-resolution stratigraphic correlation for the base of the Mont d'Hauris Fm in Belgium and France is proposed due to similar MS data established in the "Les Monts de Baileux" section 40 km apart from the stratotype area.

Acknowledgements

The research has been supported by the FRFC n° 2.4518.07 project of the Belgian "Fonds National de la Recherche Scientifique (FNRS)", and contributes to the IGCP Project n° 580 "Application of magnetic susceptibility on Paleozoic sedimentary rocks", and to the IGCP Project n° 596 "Climate change and biodiversity patterns in the Mid-Paleozoic (Early Devonian to Late Carboniferous)". The authors are grateful to Claudia Dojen of the Landesmuseum Kärnten, and to Etienne Steurbaut (KBIN) for their constructive reviews, improving the manuscript. Finally, we thank the Prefect of the Ardennes Department who authorized the access and the sampling of the studied sections at the Mont d'Hauris.

References

- ADAMCZAK, F., 1968. Palaeocopa and Platycopida (Ostracoda) from Middle Devonian rocks in the Holy Cross Mountains, Poland. *Stockholm Contributions in Geology*, **57**, 109 pp.
- ADAMCZAK, F., 1976. Middle Devonian Podocopida (Ostracoda) from Poland; their morphology, systematics and occurrence. *Senckenbergiana lethaea*, **57** (4-6): 265-467.
- AHR, W.M., 1973. The carbonate ramp : an alternative to the shelf model. *Transactions, Gulf Coast Association of Geological Societies*, **23**: 203-212.
- AIGNER, T., 1985. Storm depositional systems. Dynamic stratigraphy on modern and ancient shallow-marine sequences. *Lecture Notes in Earth Sciences*, **3**, Springer Verlag, 174 pp.
- ANDREWS, J.T. & STRAVERS, J.A., 1993. Magnetic susceptibility of late Quaternary marine sediments, Frobisher Bay, N.W.T.: an indicator of changes in provenance and process. *Quaternary Science Reviews*, **12**: 157-168.
- BANDEL, K. & BECKER, G., 1975. Ostracoden aus paläozoischen pelagischen Kalken der Karnischen Alpen (Silurium bis Unterkarbon). *Senckenbergiana lethaea*, **56** (1): 1-83.
- BECKER, G., 1964. Palaeocopida (Ostracoda) aus dem Mitteldevon der Sötenicher Mulde (N-Eifel). *Senckenbergiana lethaea*, **45** (1-4): 43-113.
- BECKER, G., 1965. Podocopida (Ostracoda) aus dem Mitteldevon der Sötenicher Mulde (N-Eifel). *Senckenbergiana lethaea*, **46** (4-6): 367-441.
- BECKER, G. & BLESS, M., 1974. Ostracode stratigraphy of the Ardenno-Rhenish Devonian and Dinantian. In: BOUCKAERT, J. & STREEL, M. (eds), Publication of the International Symposium on Belgian Micropaleontological limits, Namur, **1**, 52 pp.
- BLOEMENDAL, J., KING, J.W., TAUXE, L. & VALET, J.-P., 1989. Rock magnetic stratigraphy of Leg 108 Sites 658, 659, 661 and 665, eastern tropical Atlantic. In: RUDDIMAN, W.F. et al. (eds), Proceedings of the Ocean Drilling Program, Initial Reports, 108 (College Station, TX): 415-428.
- BOULVAIN, F., MABILLE, C., POULAIN, G., & DA SILVA, A-C., 2009. Towards a palaeogeographical and sequential framework for the Givetian of Belgium. *Geologica Belgica*, **12**: 161-178.
- BULTYNCK, P., 1987. Pelagic and neritic conodont successions from the Givetian of pre-Saharan Morocco and the Ardennes. *Bulletin de l'Institut royal des Sciences naturelles de Belgique, Sciences de la Terre*, **57**: 149-181.
- BULTYNCK, P., COEN-AUBERT, M., DEJONGHE, L., GODEFROID, J., HANCE, L., LACROIX, D., PRÉAT, A., STAINIER, P., STEEMANS, P., STEEL, M. & TOURNEUR, F., 1991. Les formations du Dévonien Moyen de la Belgique. *Mémoires pour servir à l'explication des cartes géologiques et minières de la Belgique*, **30**, 105 pp.
- BULTYNCK, P. & DEJONGHE, L., 2001. Devonian lithostratigraphic units (Belgium). *Geologica Belgica*, **4** (1-2): 39-69.
- BURCHETTE, T.P. & WRIGHT, V.P., 1992. Carbonate ramp depositional systems. In: SELLWOOD B.W. (ed.), Ramps and

- Reefs. *Sedimentary Geology*, **79**: 3-57.
- CAMBIER, G., 2010. Etude sédimentologique, magnétique et géochimique du Givetien Inférieur de Givet (formations de Trois-Fontaines et des Terres d'Haur au bord sud du synclinorium de Dinant). Master thesis, Université Libre de Bruxelles, 105 pp.
- CASIER, J.-G., 1985. Les Ostracodes de la partie supérieure de la Formation de Teferguenite (Givétien) et de la Formation de Marhouna (Givétien - Famennien) de la coupe du Km 30 (Saoura, Sahara algérien). *Géobios*, **18** (6): 833-846.
- CASIER, J.-G., 1987. Etude biostratigraphique et paléoécologique des ostracodes du récif de marbre rouge du Hautmont, à Vodelée (partie supérieure du Frasnien, Bassin de Dinant, Belgique). *Revue de Micropaléontologie*, **6** (2): 193-204.
- CASIER, J.-G., 2004. The mode of life of Devonian entomozoacean ostracods and the Myodocopid Meg-Assemblage proxy for hypoxic events. *Bulletin de l'Institut royal des Sciences naturelles de Belgique, Sciences de la Terre*, **74-suppl.**: 73-80.
- CASIER, J.-G., 2008. Guide de l'excursion: Les ostracodes du Dévonien Moyen et Supérieur du Synclinorium de Dinant. In: J.-G. CASIER (ed.), Résumé des communications et guide de l'excursion, 22^{ème} Réunion des Ostracodologues de langue française, Bruxelles 2-4 juin. Institut royal des Sciences naturelles de Belgique, 83 pp.
- CASIER, J.-G., CMBIER, G., DEVLEESCHOUWER, X., PETITCLERC, E. & PRÉAT, A., 2010. Ostracods, rock facies and magnetic susceptibility of the Trois-Fontaines and Terres d'Haur Formations (Early Givetian) in the Rancennes Quarry at the Mont d'Haur (Givet, France). *Bulletin de l'Institut royal des Sciences naturelles de Belgique, Sciences de la Terre*, **80**: 85-114.
- CASIER, J.-G., DEVLEESCHOUWER, X., PETITCLERC, E. & PRÉAT, A., 2011. Ostracods, rock facies and magnetic susceptibility of the Hanonet Formation/Trois-Fontaines Formation boundary interval (Early Givetian) at the Mont d'Haur (Givet, France). *Bulletin de l'Institut royal des Sciences naturelles de Belgique, Sciences de la Terre*, **81**: 63-96.
- CASIER, J.-G., EL HASSANI, A. & PRÉAT, A., 2010. Ostracodes du Dévonien moyen et supérieur du Tafifalt (Maroc). *Revue de Micropaléontologie*, **53**: 29-51.
- CASIER, J.-G., KASIMI, R. & PRÉAT, A., 1995. Les Ostracodes au passage Eifelien/Givetien à Glageon (Avesnois, France). *Géobios*, **28** (4): 487-499.
- CASIER, J.-G., LEHMAMI, M. & PRÉAT, A., 1997. Ostracodes et sédimentologie du Givétien à Ain Khira (Meseta nord-occidentale du Maroc). *Revue de Paléobiologie, Genève*, **16** (1): 151-167.
- CASIER J.-G. & PRÉAT, A., 1990. Sédimentologie et Ostracodes de la limite Eifelien-Givetien à Resteigne (bord sud du Bassin de Dinant, Belgique). *Bulletin de l'Institut royal des Sciences naturelles de Belgique, Sciences de la Terre*, **60**: 75-105.
- CASIER, J.-G. & PRÉAT, A., 1991. Evolution sédimentaire et Ostracodes de la base du Givetien à Resteigne (bord sud du Bassin de Dinant, Belgique). *Bulletin de l'Institut royal des Sciences naturelles de Belgique, Sciences de la Terre*, **61**: 155-177.
- CASIER J.-G. & PRÉAT, A., 2003. Ostracods and lithofacies of the Devonian-Carboniferous boundary beds in the Avesnois, North of France. *Bulletin de l'Institut royal des Sciences naturelles de Belgique, Sciences de la Terre*, **73**: 83-107.
- CASIER J.-G. & PRÉAT, A., 2006. Ostracods and lithofacies close to the Eifelian-Givetian boundary (Devonian) at Aisemont (Namur Synclinorium, Belgium). *Bulletin de l'Institut royal des Sciences naturelles de Belgique, Sciences de la Terre*, **76**: 5-29.
- CASIER, J.-G. & RACHEBOEUF, P., 2008. Ostracods from the Belen Formation at Pisacavina (Altiplano, Bolivia). In: P. KÖNIGSHOF & U. LINNEMANN (eds), Abstracts and Programme of the final meeting of IGCP 497 and IGCCP 499 - 20th International Senckenberg-Conference & 2nd Geinitz-Conference: "From Gondwana and Laurussia to Pangea: Dynamics of Oceans and Supercontinents", Frankfurt am Main (Germany): 162-163.
- CHEN, T., HUIFANG, X., XIE, Q., CHEN, J., JI, J. & LU, H., 2005. Characteristics and genesis of maghemite in Chinese loess and paleosols: mechanism for magnetic susceptibility enhancement in paleosols. *Earth and Planetary Science Letters*, **240**: 790-802.
- COEN, M., 1985. Ostracodes givétiens de l'Ardenne. *Mémoires de l'Institut géologique de l'Université de Louvain*, **32**, 48 pp.
- CRICK, R.E., ELLWOOD, B. & EL HASSANI, A., 1994. Integration of biostratigraphy, magnetic susceptibility and relative sea-level change: a new look at high resolution correlation. *Subcommission on Devonian Stratigraphy Newsletter*, **11**: 59-66.
- CRICK, R.E., ELLWOOD, B., EL HASSANI, A. & FEIST, R., 2000. Proposed magnetostratigraphy susceptibility magnetostratotype for the Eifelian-Givetian GSSP (Anti-Atlas, Morocco). *Episodes*, **23** (2): 93-101.
- CRICK, R.E., ELLWOOD, B., EL HASSANI, A., FEIST, R. & HLADIL, J., 1997. Magneto-Susceptibility Event and Cyclostratigraphy (MSEC) of the Eifelian-Givetian GSSP and associate boundary sequences in north Africa and Europe. *Episodes*, **20** (3): 167-175.
- CRICK, R.E., ELLWOOD, B.B., HLADIL, J., EL HASSANI, A., HROUDA, F. & CHLUPAC, I., 2001. Magnetostratigraphy susceptibility of the Pridolian-Lochkovian (Silurian-Devonian) GSSP (Klonk, Czech Republic) and coeval sequence in Anti-Atlas Morocco. *Palaeogeography, Palaeoclimatology, Palaeoecology*, **167**: 73-100.

- DA SILVA, A.C., MABILLE, C. & BOULVAIN, F., 2009. Influence of sedimentary setting on the use of magnetic susceptibility: examples from the Devonian of Belgium. *Sedimentology*, **56**: 1292-1306.
- DEVLEESCHOUWER, X., 1999. La limite Frasnien-Famennien (Dévonien Supérieur) en Europe: sédimentologie, stratigraphie séquentielle et susceptibilité magnétique. Université Libre de Bruxelles et Université des Sciences et Technologies de Lille, 414 pp (unpublished Doctoral thesis in French, with English abstract).
- DEVLEESCHOUWER, X., PETITCLERC, E., SPASSOV, S. & PRÉAT, A., 2010. The Givetian-Frasnian boundary at Nismes parastratotype (Belgium): the magnetic susceptibility signal controlled by ferromagnetic minerals. *Geologica Belgica*, **13** (4): 345-360.
- DEVLEESCHOUWER, X., PRÉAT, A., AVERBUCH, A. & HERBOSCH, A. 1999. Magnetic susceptibility through the Frasnian-Famennian boundary (Steinbruch Schmidt, Germany and Coumiac, France). *Abstract book 19th regional European Meeting of Sedimentology, Copenhagen, Denmark*: 71-72.
- DUNHAM, R.J., 1970. Keystone vugs in carbonate beach deposits. *American Association of Petroleum Geologists Bulletin*, **54**: 845.
- ELLWOOD, B., BENOIST, S.L., EL HASSANI, A., WHEELER, C. & CRICK, R.E., 2003. Impact ejecta layer from the Mid-Devonian: possible connection to global mass extinctions. *Science*, **300**: 1734-1737.
- ELLWOOD, B., BRETT, C.E. & MACDONALD, W.D., 2007. Magnetostratigraphy susceptibility of the Upper Ordovician Kope Formation, northern Kentucky. *Palaeogeography, Palaeoclimatology, Palaeoecology*, **243**: 42-54.
- ELLWOOD, B., CRICK, R.E. & EL HASSANI, A., 1999. The Magneto-Susceptibility Event and Cyclostratigraphy (MSEC) method used in geological correlation of Devonian rocks from Anti-Atlas Morocco. *American Association of Petroleum Geology Bulletin*, **83** (7): 1119-1134.
- ELLWOOD, B., CRICK, R.E., EL HASSANI, A., BENOIST, S.L. & YOUNG, R.H., 2000. Magnetosusceptibility event and cyclostratigraphy method applied to marine rocks: detrital input versus carbonate productivity. *Geology*, **28** (12): 1135-1138.
- ELLWOOD, B., CRICK, R.E., GARCIA-ALCALDE FERNANDEZ, J.L., SOTO, F.M., TRUYOLS-MASSONI, M., EL HASSANI, A. & KOVAS, E.J., 2001. Global correlation using magnetic susceptibility data from Lower Devonian rocks. *Geology*, **29** (7): 583-586.
- ELLWOOD, B., TOMKIN, J.H., RATCLIFFE, K.T., WRIGHT, M. & KAFAFY, A.M., 2008. High-resolution magnetic susceptibility and geochemistry for the Cenomanian/Turonian boundary GSSP with correlation to time equivalent core. *Palaeogeography, Palaeoclimatology, Palaeoecology*, **261**: 105-126.
- ERRERA, M., MAMET, B. & SARTENAER, P., 1972. Le calcaire de Givet et le Givétien à Givet. *Bulletin de l' Institut royal des Sciences naturelles de Belgique, Sciences de la Terre*, **48**, 1, 59 pp.
- ESTEBAN, M. & KLAPPA, C.F., 1983. Subaerial exposure environment. In: SCHOLLE, P.A., BEBOUT, D.G. & MOORE, C.H. (eds): Carbonate Depositional Environments. *Memoir American Association Petroleum Geologists*, **33**: 1-72.
- GARWOOD, E. J., 1931. The Tuedian beds of northern Cumberland and Roxburgshire, east of the Liddel Water. *Geological Society of London, Quarterly Journal*, **87**: 97-157.
- GORBARENKO, S.A., NUERNBERG, D., DERKACHEV, A.N., ASTAKHOV, A.S., SOUTHON, J.R. & KAISER, A., 2002. Magnetostratigraphy and tephrochronology of the upper Quaternary sediments in the Okhotsk Sea: implication of terrigenous, volcanogenic and biogenic matter supply. *Marine Geology*, **183**: 107-129.
- GROOS, H., 1969. Mitteldevonische Ostracoden zwischen Ruhr und Sieg (Rechtsrheinisches Schiefergebirge). *Göttinger Arbeiten zur Geologie und Paläontologie*, **1**, 110 p.
- GUERNET, C. & LETHIERS, F., 1989. Ostracodes et recherche des milieux anciens: possibilités et limites. *Bulletin de la Société géologique de France*, **8** (3): 577-588.
- HINE, A.C., WILBER, R.J. & NEUMANN, A.C., 1981. Carbonate sand bodies along contrasting shallow bank margins facing open ocean seaways in northern Bahamas. *American Association Petroleum Geologists Bulletin*, **65**: 261-290.
- HLADIL, J., 2002. Geophysical records of dispersed weathering products on the Frasnian carbonate platform and early Famennian ramps in Moravia, Czech Republic: proxies for eustasy and paleoclimate. *Palaeogeography, Palaeoclimatology, Palaeoecology*, **181**: 213-250.
- HLADIL, J., GERSL, M., STRNAD, L., FRANA, J., LANGROVA, A. & SPISIAK, J., 2006. Stratigraphic variation of complex impurities in platform limestones and possible significance of atmospheric dust: a study with emphasis on gamma-ray spectrometry and magnetic susceptibility outcrop logging (Eifelian-Frasnian, Moravia, Czech Republic). *International Journal of Earth Sciences*, **95**: 703-723.
- HORBURY, A.D., 1992. A Late Dinantian peloid cementstone-palaeoberesellid buildup from North Lancashire, England. *Sedimentary Geology*, **79**: 17-137.
- HUBERT, B., 2008. Detailed lithology and faunal occurrence of the historical Givetian section: the fortifications of the Mont d'Haurs (Givet, France). *Annales de la Société géologique du Nord*, **15**, 2^{ème} sér.: 53-65.
- KASIMI, R. & PRÉAT, A., 1996. Sédimentation de rampe mixte silico-carbonatée des couches de transition eiféliennes-givétiennes franco-belges. Deuxième partie:

- Cyclostratigraphie et paléostructuration. *Bulletin Centres Rech.-Prod. Elf Aquitaine*, **20**: 62-90.
- KEGEL, W., 1932. Zur Kenntnis paläozoischer Ostrakoden 2. Bairdiidae aus dem Mitteldevon des Rheinischen Schiefergebirges. *Jahrbuch der Preussischen Geologischen Landesanstalt zu Berlin*, **52** (1931): 245-250.
- KRÖMMELBEIN, K., 1952. Ostrakoden-Studien im Devon der Eifel - 2: Die Taxonomische Stellung der Gattung *Bairdia* MC COY im Mittel-Devon. *Senckenbergiana*, **31** (5-6): 331-338.
- KRÖMMELBEIN, K., 1953. Ostrakoden-Studien im Devon der Eifel - 3: Nachweis der polnischen Gattungen *Polyzygia* und *Poloniella* im Mittel-Devon der Eifel. *Senckenbergiana*, **34** (1-3): 53-59.
- KUMMEROW, E., 1953. Über oberkarbonische und devonische Ostrakoden in Deutschland und in der Volksrepublik Polen. *Geologie*, **7**, 75 pp.
- LETHIERS, F. & CRASQUIN-SOLEAU, S., 1988. Comment extraire les microfossiles à tests calcitiques des roches calcaires dures. *Revue de Micropaléontologie*, **31** (1): 56-61.
- LETHIERS, F., RACHEBOEUF, P., BAUDIN, F. & VACCARI, E., 2001. A typical Malvinokaffric Givetian ostracod fauna from Bolivia. *Revue de Micropaleontology*, **44** (4): 301-317.
- MABILLE, C., 2008. Dynamique sédimentaire de l'Eifelien et de la base du Givetien en Belgique et dans les régions limitrophes. Thèse de Doctorat inédite, Université de Liège, 185 pp.
- MABILLE, C. & BOULVAIN, F., 2008. Les Monts de Baileux section: detailed sedimentology and magnetic susceptibility of Hanonet, Trois-Fontaines and Terres d'Haur Formations (Eifelian/Givetian boundary and Lower Givetian, SW Belgium). *Geologica Belgica*, **11**: 93-121.
- MAGNE, F., 1964. Données micropaléontologiques et stratigraphiques dans le Dévonien du Boulonnais (France) et du Bassin de Namur (Belgique). Thèse de 3^{ème} cycle, Université de Paris, Société nationale des Pétroles d'Aquitaine, Centre de Recherches de Pau, 172 pp.
- MAMET, B. & PRÉAT, A., 2005. Sédimentologie de la série viséenne d'Avesnes-sur-Helpe (Avesnois, Nord de la France). *Geologica Belgica*, **8**: 9-107.
- MILHAU, B., 1983. Ostracodes du Givétien supérieur du Boulonnais. Corrélations avec l'Ardenne. *Annales de la Société géologique du Nord*, **102**: 217-236.
- OLEMPSKA, E., 1979. Middle to Upper Devonian Ostracoda from the Southern Holy Cross Mountains, Poland. *Palaeontologica Polonica*, **40**: 57-162.
- POKORNY, V., 1950. Skorepatci strednodevonskych "cervenyh vapencu koralovych" z Celechovic. *Sbornik Statniho Geologickeho Ustavu Ceskoslovenske Republiky*, **17 Odil Paleontologicky**: 513-632.
- POLENOVA, E., 1955. Ostrakody Devona Volgo-Uralskoy Oblasti. *Trudy Vsesoyuznogo Neftyanogo Nauchno-issledovatel'skogo Geologo-razvedochnogo Instituta (VNIGRI), Novaya seriya*: 191-287.
- PONOMAREV, V.N. & NECHOROSHKOV, L., 1984. Downhole magnetic measurements in oceanic crustal hole 395A on the Mid-Atlantic Ridge. In: HYNDMAN, R.D. et al. (eds), Initial Reports on DSDP, **78b**, Washington, 731-739.
- PRÉAT, A. & KASIMI, R., 1995. Sédimentation de rampe mixte silico-carbonatée des couches de transition eiféliennes-givétienne franco-belges. Première partie: microfaciès et modèle sédimentaire. *Bulletin Centres Rech.-Prod. Elf Aquitaine*, **19**: 329-375.
- PRÉAT, A. & MAMET, B., 1989. Sédimentation de la plate-forme carbonatée givétienne franco-belge. *Bulletin Centres Rech.-Prod. Elf Aquitaine*, **13**: 47-86.
- RIQUIER, L., AVERBUCH, O., DEVLEESCHOUWER, X. & TRIBOVILLARD, N., 2010. Rock magnetic evidences for a major climatic transition at the Frasnian-Famennian boundary (ca 375 Ma BP). *International Journal of Earth Sciences*, **99**: S57-S73. DOI 10.1007/s00531-009-0492-7.
- ROBINSON, S.G., 1993. Lithostratigraphic applications for magnetic susceptibility logging of deep sea sediment cores: examples from ODP Leg 115. In: HAILWOOD, E.A. & KIDD, R.B. (eds), High Resolution Stratigraphy. *Geological Society of London, Special Publication*, **70**: 65-98.
- ROZHDESTVENSKAJA, A., 1959. Ostrakody terrigennoy tolshchi Devona zapadnoy Bashkirii i ikh stratigraficheskoe znachenie. In: CHRIBIKOVA, E. & ROZHDESTVENSKAJA, A. (eds), Materialy po paleontologii i stratigrafiyi Devonskikh i bolee drevnikh otlozheniy Bashkirii: 117-247.
- ROZHDESTVENSKAJA, A., 1962. Srednedevonskie ostrakody zapadnogo sklona yuzhnogo Urala, Preduralkogo progiba i platformennoy chasti Bashkirii. In: THYAZHEVA, A., ROZHDESTVENSKAJA, A. & CHIRIBIKOVA, E. (eds), Brakhiopody, Ostrakody i spory srednego i verkhnego Devona Bashkirii: 169-349.
- VANDERAVEROET, P., AVERBUCH, O., DECONINCK, J.-F. & CHAMLEY, H., 1999. Glacial/interglacial cycles in Pleistocene sediments of New Jersey expressed by clay minerals, grainsize and magnetic susceptibility data. *Marine Geology*, **159**: 79-92.
- VAN WAGONER, J., MITCHUM, R., POSAMENTIER, H. & VAIL, P., 1987. Seismic stratigraphy interpretation using sequence stratigraphy. Part II: the key definition of sequence stratigraphy. In: BALLY, A. (ed.), *Atlas of seismic stratigraphy 1. American Association Petroleum Geologists Studies Geology*, **27**: 11-14.
- WAHLMAN, G.P., 2010. Reflux dolomite crystal size variation in cyclic inner ramp reservoir facies, Bromide Formation (Ordovician), Arkoma Basin, Southeastern Oklahoma. *The Sedimentary Record*, **8**: 4-9.
- ZAGORA, K., 1968. Ostracoden aus dem Grenzbereich

Unter-/Mitteldevon von Ostthueringen. *Geologie, Jahrgang 17, Beiheft, 62:* 1-91.

ZBIKOWSKA, B., 1983. Middle to Upper Devonian Ostracods from northwestern Poland and their stratigraphic significance. *Palaeontologica Polonica, 44,* 108 pp.

Julien MOREAU

Département des Sciences de la Terre et de l'Environnement

Université libre de Bruxelles CP 160

Av. F. D. Roosevelt, 50, B-1050 Bruxelles, Belgique

E-mail: jmoreau@ulb.ac.be

Estelle PETITCLERC

Service géologique de Belgique

Institut royal des Sciences naturelles de Belgique

Rue Jenner, 13, B-1000 Bruxelles, Belgique

E-mail: estelle.petitclerc@naturalsciences.be

Alain PRÉAT

Département des Sciences de la Terre et de l'Environnement

Université libre de Bruxelles CP 160

Av. F. D. Roosevelt, 50, B-1050 Bruxelles, Belgique

E-mail: apreat@ulb.ac.be

Typescript submitted: June 5, 2011

Revised typescript received: September 6, 2011

Explanation of plates

The types are deposited in the collections of the Department of Paleontology (section Micropaleontology) of the Royal Belgian Institute of Natural Sciences (IRScNB n° b 58...). The thin sections are deposited in the Department of Earth Sciences and Environment of the University of Brussels (ulb/sed ...). MH = sample number (see Fig. 2 for the stratigraphic position), TH Fm = Terres d'Haur Fm; MH Fm = Mont d'Haur Fm.

PLATE 1

- Fig. 1 — *Amphissites tener* BECKER, 1964, MH-400, TH Fm, IRScNB n° b5840, right lateral view of a carapace, x65.
- Fig. 2 — *Parabolbinella coeni* CASIER, 2011, MH-332, TH Fm, IRScNB n° b5841, right lateral view of a carapace. x60.
- Fig. 3 — *Ctenoloculina* sp. A, aff. *kelletae* POKORNY, 1950, MH-333, TH Fm, IRScNB n° b5842, left lateral view of a broken carapace x65.
- Fig. 4 — *Kozlowskiella? rugulosa* (KUMMEROW, 1953), MH-227, TH Fm, IRScNB n° b5843, right valve slightly tipped up, x55.
- Fig. 5 — *Kozlowskiella* sp. C, MH-309, TH Fm, IRScNB n° b5844, right valve, x55.
- Fig. 6 — *Kozlowskiella* sp. A sensu BECKER, 1964, MH-309, TH Fm, IRScNB n° b5845, right lateral view of a carapace, x50.
- Fig. 7 — “*Kozlowskiella*” sp. B, MH-243, TH Fm, IRScNB n° b5846, right lateral view of a carapace, x80.
- Fig. 8 — *Parapribilites hanaicus* POKORNY, 1950, MH-239, TH Fm, IRScNB n° b5847, left lateral view of a carapace, x85.
- Fig. 9 — *Kielciella fastigans* (BECKER, 1964), MH-267, TH Fm, IRScNB n° b5848, right lateral view of a broken carapace, x60
- Fig. 10 — *Kielciella* cf. *arduennensis* ADAMCZAK & COEN, 1992, MH-417, MH Fm, IRScNB n° b5849, left lateral view of a poorly preserved carapace, x40.
- Fig. 11 — *Roundyella patagiata* (BECKER, 1964), MH-429, MH Fm, IRScNB n° b5850, lateral view of a carapace, x80.
- Fig. 12 — “*Aparchites*” sp. indet., MH-436, MH Fm, IRScNB n° b5851, right lateral view of a carapace, x60.
- Fig. 13 — *Buregia ovata* (KUMMEROW, 1953), MH-221, TH Fm, IRScNB n° b5852, left lateral view of a carapace, x45.
- Fig. 14 — Hollinidae gen. and sp. indet. 1, MH-221, TH Fm, IRScNB n° b5853, poorly preserved left valve, x70.
- Fig. 15 — *Coeloenellina minima* (KUMMEROW, 1953), MH-249, TH Fm, IRScNB n° b5854, right lateral view of a carapace, x90.

PLATE 2

- Fig. 1 — *Coeloenellina vellicata* COEN, 1985, MH-417, TH Fm, IRSNB n° b5855, left lateral view of a carapace, x100.
- Fig. 2 — *Samarella* n. sp., aff. *laevinodosa* POLENOVA, 1952 *sensu* CASIER & PRÉAT, 1991, MH-429, MH Fm, IRSNB n° b5856, left lateral view of a carapace, x65.
- Fig. 3 — *Samarella?* sp. A, MH-422, MH Fm, IRSNB n° b5857, left lateral view of a carapace, x55.
- Fig. 4 — *Poloniella tertia* KRÖMMELBEIN, 1953, MH-333, TH Fm, IRSNB n° b5858, left lateral view of a carapace, x50.
- Fig. 5 — *Poloniella claviformis* (KUMMEROW, 1953), MH-298, TH Fm, IRSNB n° b5859, left lateral view of a carapace, x55.
- Fig. 6 — *Marginia sculpta multicostata* POLENOVA, 1952, MH-341, TH Fm, IRSNB n° b5860, left lateral view of a carapace, x75.
- Fig. 7 — *Uchtovia abundans* (POKORNY, 1950), MH-417, TH Fm, IRSNB n° b5861, left lateral view of a carapace, x55.
- Fig. 8 — *Uchtovia refrathensis* (KRÖMMELBEIN, 1954), MH-400, TH Fm, IRSNB n° b5862, right lateral view of a carapace, x60.
- Fig. 9 — *Evlanelia germanica* BECKER, 1964, MH-249, TH Fm, IRSNB n° b5863, right lateral view of a carapace, x75.
- Fig. 10 — *Evlanelia mitis* ADAMCZAK, 1968, MH-341, TH Fm, IRSNB n° b5864, right lateral view of a carapace, x70.
- Fig. 11 — *Evlanelia cf. lessensis* CASIER, 1991, MH-289, TH Fm, IRSNB n° b5865, left lateral view of a carapace, x75.
- Fig. 12 — *Cavellina devoniana* EGOROV, 1950, MH-417, TH Fm, IRSNB n° b5866, left lateral view of a carapace, x65.
- Fig. 13 — *Cavellina cf. rhenana* KRÖMMELBEIN, 1954, MH-239, MH Fm, IRSNB n° b5867, left lateral view of a carapace, x40.
- Fig. 14 — *Buflina schaderthalensis* ZAGORA, 1968, MH-408, MH Fm, IRSNB n° b5868, right lateral view of a carapace, x55.
- Fig. 15 — *Ropolonellus kettneri* (POKORNY, 1950), MH-417, MH Fm, IRSNB n° b5869, right lateral view of a carapace, x85.

PLATE 3

- Fig. 1 — *Cytherellina* sp. A, aff. *obliqua* (KUMMEROW, 1953), MH-239, MH Fm, IRSNB n° b5870, right lateral view of a carapace, x85.
- Fig. 2 — *Cytherellina obliqua* (KUMMEROW, 1953), MH-400, MH Fm, IRSNB n° b5871, right lateral view of a carapace, x70.
- Fig. 3 — *Cytherellina* sp. B, aff. *obliqua* (KUMMEROW, 1953), MH-201, MH Fm, IRSNB n° b5872, right lateral view of a carapace, x60.
- Fig. 4 — *Cytherellina perlonga* (KUMMEROW, 1953), MH-429, MH Fm, IRSNB n° b5873, right lateral view of a carapace, x60.
- Fig. 5 — *Jenningsina heddebauti* MILHAU, 1983, MH-404, TH Fm, IRSNB n° b5874, right lateral view of a carapace, x90.
- Fig. 6 — *Jefina romei* COEN, 1985?, MH-201, TH Fm, IRSNB n° b5875, right lateral view of a carapace, x80.
- Fig. 7 — *Quasillites fromelennensis* MILHAU, 1983, MH-298, TH Fm, IRSNB n° b5876, right lateral view of a carapace, x55.
- Fig. 8 — *Polyzygia symmetrica* GÜRICH, 1896, MH-201, TH Fm, IRSNB n° b5877, poorly preserved right valve, x85.
- Fig. 9 — *Zeuschnerina dispar* ADAMCZAK, 1976. MH-422, MH Fm, IRSNB n° b5878, poorly preserved right valve, x75.
- Fig. 10 — *Bairdiocypris rauffi* KRÖMMELBEIN, 1952, MH-417, TH Fm, IRSNB n° b5879, right lateral view of a carapace, x25.
- Fig. 11 — *Acratia lucea* MAILLET, 2010 *nom. nud.*, MH-341, TH Fm, IRSNB n° b5880, right lateral view of a broken carapace, x70.
- Fig. 12 — “*Healdianella*” *budensis* OLEMPSKA, 1979, MH-298, TH Fm, IRSNB n° b5881, right lateral view of a carapace, x50.
- Fig. 13 — *Orthocypris cicatricosa* COEN, 1985, MH-332, TH Fm, IRSNB n° b5882, right lateral view of a carapace, x75.
- Fig. 14 — “*Orthocypris*” sp. indet. 1, MH-413, TH Fm, IRSNB n° b5883, right lateral view of a carapace, x70.
- Fig. 15 — “*Orthocypris*” sp. indet. 2, MH-341, TH Fm, IRSNB n° b5884, right lateral view of a carapace, x70.
- Fig. 16 — *Tubilibairdia clava* (KEGEL, 1932), MH-400, TH Fm, IRSNB n° b5885, right lateral view of a carapace, x50.

- Fig. 17 — *Bairdia cf. paffrathensis* KUMMEROW, 1953, MH-201, TH Fm, IRSNB n° b5886, right lateral view of a carapace, x50.
- Fig. 18 — *Bairdia paffrathensis* KUMMEROW, 1953, MH-417, TH Fm, IRSNB n° b5887, right lateral view of a carapace, x50.

PLATE 4

- Fig. 1 — Argillaceous silty bioturbated bioclastic mudstone. Strongly altered crinoidal fragment with two thin molluscan shells. MH-349, 8810/2011/ulb, MF1, TH Fm.
- Fig. 2 — Argillaceous silty bioturbated bioclastic wackestone with trilobite, echinoderms, ostracods and various thin shells. The bioclasts form a thin tempestite layer which has been slightly bioturbated (see text). MH-349, 8809/2011/ulb, MF1, TH Fm.
- Figs 3-4 — Peloidal bioclastic wackestone with echinodermal pieces (Fig. 4), ostracod carapaces, thin pelecypod shells and kamaenid fragments forming a tempestite layer (see text). A few micritized grains are present. MH-339, respectively 8811/2011/ulb and 8813/2011/ulb, MF2, TH Fm.
- Fig. 5 — Heavily burrowed packstone with abundant bioclasts (kamaenid at the centre of the picture, echinoderms and thin-shelled pelecypods). The micritic matrix is slightly microsparitized. MH-292, 8345/2011/ulb, MF3, TH Fm.
- Fig. 6 — Heavily burrowed bioclastic packstone with an archaeogastropod and a few oolites. MH-256, 7476/2011/ulb, MF3, TH Fm.
- Figs 7-8 — Bioclastic peloidal packstone with abundant gastropods and pelecypods (Fig. 7) and well delimited burrows filled with a very fine-grained bioclastic packstone. MH-292, respectively 8343/2011/ulb and 8344/2011/ulb, MF3, TH Fm.

PLATE 5

- Fig. 1 — Peloidal bioclastic packstone with encrusting bryozoans and thin molluscan shells. Palaeoberesellids are dispersed in the micrite matrix (example in the upper right corner). MH-233, 8326/2011/ulb, MF4, TH Fm.
- Figs 2, 4 — Bioclastic grainstone with a floated goniatite inside a gastropod (Fig. 4), kamaenids, ostracods, echinoderms, and irregular micobreccias with a syntaxial calcite cement (Fig. 4). The coarse-grained bioclasts constitute a proximal tempestite (see text). MH-234, respectively 8329/2011/ulb and 7517/2011/ulb, MF4, TH Fm.
- Fig. 3 — Bioturbated packstone with a large irregular micobreccia consisting of bioclastic (with stacked ostracod carapaces, pelecypods and palaeoberesellids) wackestone/packstone. MH-236, 8330/2011/ulb, MF4, TH Fm.
- Fig. 5 — Coral (tabulata) floatstone with a burrowed peloidal microbioclastic micritic matrix. MH-242, 7492/2011/ulb, MF5, TH Fm.
- Fig. 6 — Stromatopore-coral rudstone. The organisms are mutually encrusted. MH-323, 8808/2011/ulb, MF5, TH Fm.
- Fig. 7 — Bryozoan grainstone with various micritized bioclasts of echinoderms and molluscs. Syntaxial cementation is present. MH-261, 7460/2011/ulb, MF6, TH Fm.
- Fig. 8 — Oolitic grainstone with a few micritized bioclasts, micritized grains and peloids. MH-317, 8805/2011/ulb, MF6, TH Fm.

PLATE 6

- Fig. 1 — Well-sorted peloidal algal (issinellids and kamaenids) grainstone with a few micritized grains. MH-202, 8320/2011/ulb, MF7, TH Fm.
- Fig. 2 — Well-sorted laminar issinellid packstone with a partly microsparitized micritic matrix (“false cement”, see text). MH-247, 8318/2011/ulb, MF7, TH Fm.
- Figs 3-4 — Issinellid baffestone. MH-267, respectively 7441/2011/ulb and 7443/2011/ulb, MF8, TH Fm.
- Figs 5-6 — Algal (palaeoberesellids) wackestone with microbioclasts and ostracods (Fig. 5) and large-sized *Bevocastria* nodule (Fig. 6) in a homogeneous micritic matrix. MH-212, respectively 7543/2011/ulb and 7539/2011/ulb, MF9, TH Fm.
- Figs 7-8 — Packstone with poorly sorted micobreccia consisting of a lumpy mudstone (Fig. 7) and laminar ostracod wackestone/packstone with desiccation cracks (Fig. 8). The large-sized micobreccias are surrounded or not (quadrangular). Microbioclasts are present in the micritic matrix. MH-271, respectively 7421/2011/ulb and 7422/2011/ulb, MF10, TH Fm.

